The Journal of Immunology

Tumor Tolerance–Promoting Function of Regulatory T Cells Is Optimized by CD28, but Strictly Dependent on Calcineurin

Francesco Marangoni, Ruan Zhang, Vinidhra Mani, Martin Thelen, Noor J. Ali Akbar, Ross D. Warner, Tarmo Äijö, Valentina Zappulli, Gustavo J. Martinez, Laurence A. Turka and Thorsten R. Mempel

J Immunol published online 16 April 2018
http://www.jimmunol.org/content/early/2018/04/14/jimmunol.1701220

Supplementary Material **http://www.jimmunol.org/content/suppl/2018/04/14/jimmunol.1701220.DCSupplemental**

The Journal of Immunology is published twice each month by
The American Association of Immunologists, Inc.,
1451 Rockville Pike, Suite 650, Rockville, MD 20852

Print ISSN: 0022-1767 Online ISSN: 1550-6606.

Published April 16, 2018, doi:10.4049/jimmunol.1701220

Tumor Tolerance–Promoting Function of Regulatory T Cells Is Optimized by CD28, but Strictly Dependent on Calcineurin

Francesco Marangoni,*,† Ruan Zhang,‡ Vinidhra Mani,*,† Martin Thelen,* Noor J. Ali Akbar,* Ross D. Warner,* Tarmo Äijö,§ Valentina Zappulli,¶ Gustavo J. Martinez,‖ Laurence A. Turka,†,‡ and Thorsten R. Mempel*,†

Regulatory T cells (Treg) restrain immune responses against malignant tumors, but their global depletion in cancer patients will likely be limited by systemic autoimmune toxicity. Instead, approaches to "tune" their activities may allow for preferential targeting of tumor-reactive Treg. Although Ag recognition regulates Treg function, the roles of individual TCR-dependent signaling pathways in enabling Treg to promote tumor tolerance are not well characterized. In this study, we examined in mouse tumor models the role of calcineurin, a key mediator of TCR signaling, and the role of the costimulatory receptor CD28 in the differentiation of resting central Treg into effector Treg endowed with tumor tropism. We find that calcineurin, although largely dispensable for suppressive activity in vitro, is essential for upregulation of ICOS and CTLA-4 in Treg, as well as for expression of chemokine receptors driving their accumulation in tumors. In contrast, CD28 is not critical, but optimizes the formation of tumor-homing Treg and their fitness in tumor tissue. Accordingly, although deletion of either CnB or CD28 strongly impairs Treg-mediated tumor tolerance, lack of CnB has an even more pronounced impact than lack of CD28. Hence, our studies reveal distinct roles for what has classically been defined as signal 1 and signal 2 of conventional T cell activation in the context of Treg-mediated tumor tolerance. ***The Journal of Immunology*****, 2018, 200: 000–000.**

CD4$^+$ Foxp3$^+$ regulatory T cells (Treg) play an essential role in maintaining immune homeostasis and regulating antipathogen responses, but their physiological functions also restrict immune responses against malignant tumors and thus promote tumor progression (1). Therapeutic depletion of Treg enhances immunological tumor control in preclinical models, but sustained and effective depletion in cancer patients is predictably limited by the ensuing systemic autoimmunity. More selective approaches are needed to target specifically those Treg that are engaged in the antitumor response. This will not only require Treg-selective drug targeting approaches, but also an understanding of the pathways that regulate the maintenance and functions of different populations of Treg at various states of activation and in different tissues.

Treg are composed of subpopulations with different migration patterns (2, 3). CD44^{low} "resting" or "central" Treg (cTreg) express the homing receptors CD62L and CCR7 and recirculate through secondary lymphoid organs (SLOs). In contrast, CD44^{hi} "activated" or "effector" Treg (eTreg) lack CD62L and CCR7, but proliferate more rapidly and express chemokine receptors that endow them with the ability to enter nonlymphoid and inflamed tissues. They also express elevated levels of proteins required for their maintenance and suppressive function, such as ICOS and CTLA-4. Treg that newly emerge from thymic development have a cTreg phenotype and can give rise to eTreg, whereas eTreg are not able to revert to cTreg (3, 4). cTreg to eTreg conversion occurs during immune homeostasis, depends on cognate Ag recognition, and is enhanced by inflammatory signals (3). During antitumor responses, self Ag-specific Treg rapidly expand in tumor-draining lymph nodes (tdLNs) in an MHC II–dependent manner (5). Treg found in tumor tissue phenotypically resemble eTreg and are highly suppressive (6).

We have previously investigated Treg responses to tumor growth by tracking TCR-transgenic clonal Treg populations and found that TCR-driven activation of cTreg in tdLNs is a prerequisite for their subsequent migration to tumors (7). We also observed that upon entry into tumor tissue, only those eTreg that locally re-encounter their cognate Ag are able to regulate the function of tumor-infiltrating CTL and prevent tumor rejection (7). Therefore, Treg depend on TCR signals both at immune induction sites for Treg activation and at immune effector sites for their suppressive

*Center for Immunology and Inflammatory Diseases, Massachusetts General Hospital, Boston, MA 02114; †Harvard Medical School, Boston, MA 02115; ‡Center for Transplantation Sciences, Massachusetts General Hospital, Boston, MA 02114; §Center for Computational Biology, Flatiron Institute, New York, NY 10010; ¶Department of Comparative Biomedicine and Food Science, University of Padua, 35020 Legnaro, Padua, Italy; and ‖Department of Microbiology and Immunology, Chicago Medical School, Rosalind Franklin University of Medicine and Science, North Chicago, IL 60064

ORCIDs: 0000-0002-2490-849X (F.M.); 0000-0002-1689-8391 (V.M.); 0000-0002-2785-9726 (M.T.); 0000-0001-6203-0190 (V.Z.); 0000-0001-8635-5424 (T.R.M.).

Received for publication August 25, 2017. Accepted for publication March 13, 2018.

This work was supported by a fellowship from the Sara Elizabeth O'Brien Foundation and the Charles King Trust (to F.M.), by a Fulbright fellowship (to V.Z.), by National Institutes of Health Grants T32CA207201 (to V.M.), AI037691 and HL018646 (to L.A.T.), and by National Institutes of Health Grants AI097052, CA150975, and CA179563 as well as the Bristol-Myers Squibb Melanoma Research Alliance Established Investigator Award in Immunotherapy (to T.R.M.).

F.M. designed and performed experiments, analyzed and interpreted data, and wrote the manuscript; R.Z., V.M., M.T., V.Z., R.D.W., and N.J.A.A. performed experiments; T.Ä. and G.J.M. analyzed chromatin immunoprecipitation sequencing data; L.A.T. provided CD28 ΔTreg mice; and T.R.M. provided overall project supervision, designed the experiments, and wrote the manuscript.

Address correspondence and reprint requests to Dr. Thorsten R. Mempel and Dr. Francesco Marangoni, Massachusetts General Hospital, 149 Thirteenth Street, Room 8301, Boston, MA 02129. E-mail addresses: tmempel@mgh.harvard.edu (T.R.M.) and marangoni.francesco@mgh.harvard.edu (F.M.)

The online version of this article contains supplemental material.

Abbreviations used in this article: cTreg, central Treg; CTV, CellTrace Violet; eTreg, effector Treg; HA, hemagglutinin; LN, lymph node; MFI, mean fluorescence intensity; PFA, paraformaldehyde; SLO, secondary lymphoid organ; tdLN, tumor-draining LN; Treg, regulatory T cell; TSS, transcription start site; WT, wild-type.

activity. In further support of a role of TCR signals in regulating cTreg to eTreg differentiation, genetic deletion of TCRs in mature, polyclonal Treg has a greater impact on the maintenance and gene expression pattern of eTreg than cTreg (8, 9). These observations support a scenario whereby TCR signals, potentially in concert with effector T cell–derived IL-2 (2, 3, 5, 10–12), induce cTreg to differentiate into eTreg and sustain their suppressive activity (2–4, 13). In addition, CD28 costimulation, which both complements and amplifies TCR signals and promotes cell survival, is not only essential for thymic Treg development, but also important for optimal Treg function, because mice with targeted deletion of CD28 in mature Treg slowly develop autoimmunity (14–16).

Although the general importance of TCR signals for Treg function is therefore established, the role of various signaling pathways activated by the TCR and costimulatory receptors for their ability to promote immune tolerance is less clear. Differences in the signaling response of Treg and conventional T cells to TCR stimulation have been noted (17–19), but whether they differ in their dependence on specific pathways for their functions in vivo, and which pathways regulate which functions of mature Treg, is unknown.

A major TCR-dependent pathway essential for effector T cell differentiation and function is Ca^{2+}- and calcineurin-dependent NFAT activation. Classic studies on calcineurin inhibitor therapy showed that calcineurin supports Treg suppressive activity in vivo, but were unable to separate a direct inhibitory effect on Treg from indirect effects, for example, through blockade of IL-2 production by conventional T cells or APCs (20). Meanwhile, reports of residual suppressive activity in Treg lacking one or two of the three T cell–expressed NFAT family proteins (NFAT1, 2, and 4) put the importance of this pathway into question (21–23). In addition, other studies suggested that NFAT activity in Treg is at least partly TCR-independent and constitutive (24, 25).

In this study we have used genetic deletion of the regulatory B subunit of calcineurin (CnB) or of CD28 specifically in mature Treg to investigate their role in the activation and differentiation of eTreg that promote tumor tolerance. We found that without CnB, Treg are unable to activate NFAT1 and 2. Although their suppressive activity is only marginally reduced in vitro, and their numbers at least in peripheral lymph nodes (LNs) are comparable to wild-type (WT) mice, CnB-deficient Treg fail to maintain immunological tolerance, to differentiate into tumor-homing eTreg, and to suppress immune responses against aggressive tumors, which as a result are controlled without additional intervention. CD28, on the other hand, in contrast to its essential role on the activation of conventional T cells, is not critical for the formation, but augments the fitness of tumor-homing eTreg. Accordingly, CD28 deletion in Treg does not abrogate, but considerably reduces their ability to promote tumor growth. Our findings identify an essential role for calcineurin to activate NFAT proteins in Treg and induce TCR-dependent expression of genes that characterize the transition from cTreg to tumor-homing eTreg. CD28, on the other hand, enables tumor tolerance through a fitness-optimizing role in eTreg.

Materials and Methods

Mice

$CnB^{fl/fl}$ (26), $Foxp3^{YFP\text{-}Cre}$ (27), $Foxp3^{CreERT2}$ (28), $Foxp3^{DTR}$ (29), $TCR\alpha^{-/-}$, C57BL/6, and BALB/c mice were from Jackson Laboratories. $CD28^{fl/fl}$ mice and pgk-HA × TCR-HA double-transgenic mice as a source of hemagglutinin (HA)-specific Treg were previously described (14, 30). All animals were housed, bred, enrolled in authorized experiments, and euthanized according to the guidelines of the Institutional Animal Care and Use Committee at Massachusetts General Hospital. In particular, animals were euthanized when mandated by a reduced state of health, with guidance from veterinary staff. The age at euthanasia was recorded in Kaplan–Meier plots.

Tumor growth studies

Tumor growth was longitudinally measured following s.c. injection into the flank of mice of 3–5 × 10^5 MCA-205, 10^6 MC38, or 10^6 CT26-HA tumor cells.

To delete floxed CnB or CD28 genes in $CnB^{fl/fl}$ × $Foxp3^{CreERT2}$ or $CD28^{fl/fl}$ × $Foxp3^{CreERT2}$ mice, 1 mg tamoxifen (Sigma-Aldrich) dissolved in 10% ethanol/90% olive oil was injected i.p. for five consecutive days.

To create mixed bone marrow chimeras, 6 × 10^6 bone marrow cells from $Foxp3^{DTR}$ mice were injected together with 12 × 10^6 bone marrow cells from CnB ΔTreg, CD28 ΔTreg, or $Foxp3^{YFP\text{-}Cre}$ mice into $TCR\alpha^{-/-}$ hosts irradiated with 400 rad. After 8 wk, healthy mice were implanted with tumors and received diphtheria toxin (Calbiochem) i.p. at 25 μg/kg on the first day, followed by daily injections of 5 μg/kg.

In vitro Treg suppression and proliferation assays

Single cell suspensions from spleen and LNs of CnB $\Delta Treg^{het}$, CD28 $\Delta Treg^{het}$, or $Foxp3^{YFP\text{-}Cre/wt}$ mice were enriched for Treg through immunomagnetic selection of $CD4^+$ $CD25^+$ cells (Miltenyi). YFP^+ $CD44^{low}$ $CD62L^{hi}$ cTreg and YFP^+ $CD44^{hi}$ $CD62L^{neg}$ eTreg were further purified by FACS. Varying numbers of cTreg or eTreg were added to 2.5 × 10^4 T cell–depleted splenocytes as APCs and 1 × 10^4 $CD4^+$ $CD25^-$ T cells labeled with 5 μM CellTrace Violet (CTV) as responder cells, and stimulated with 250 ng/ml of anti-CD3 mAb (clone 145-2c11; BioLegend). Responder cell proliferation (CTV dilution) and absolute numbers of remaining Treg was read out after 72 h. To quantify proliferation, we extrapolated the number of progenitor cells giving rise to each CTV peak by dividing the number of cells in each peak by the number of cells that would have originated from a single precursor (e.g., four cells in the peak corresponding to two divisions would have derived from one progenitor). To compute the T cell fold increase, we then divided the total number of recorded Treg by the extrapolated total number of progenitors. Percentage of suppression was scaled from 0 (proliferation of responders in absence of Treg) to 100 (complete absence of proliferation).

To follow cTreg proliferation, an identical assay was set up, but Treg, not responder T cells, were labeled with CTV.

Flow cytometric phosphoprotein analysis

Pooled splenocytes and LN cells were prestained with anti-CD25 BV421 mAbs (PC61; BioLegend) and stimulated at 37˚C using plate-immobilized anti-CD3 (10 μg/ml, clone 145-2c11) and soluble anti-CD28 (10 μg/ml, clone 37.51) Abs. At different time points, aliquots were quickly transferred into a 2-fold excess of 4% paraformaldehyde (PFA), yielding a final PFA concentration of 2.6%, incubated at room temperature for 10 min, and washed in PBS/0.5% BSA. Cells were permeabilized by dropwise addition of 1 ml ice-cold methanol and incubation on ice for 20 min, then carefully washed twice in PBS/0.5% BSA. Staining for CD4 (100 ng/ml, GK1.5; BioLegend), YFP (Alexa Fluor 488–conjugated anti-GFP/YFP polyclonal rabbit IgG; Life Technologies), Foxp3 (FJK-16s; eBioscience), pERK Thr202/Tyr204 (197G2; Cell Signaling), pS6 Ser235/236 (D57.2.2E; Cell Signaling), and IκB (L35A5; Cell Signaling) was performed at room temperature for 1 h, followed by careful washing. For quantification, we calculated the percentage of marker-positive (pERK) or -negative (IκB) cells. For pS6, we calculated the product of percentage of positive cells and mean fluorescence intensity (MFI) of positive cells (referred to as MFI*) (30) to account for both the frequency of signaling cells and their content of phosphoprotein. To permit comparisons across experiments, we normalized each parameter in individual experiments by assigning a value of 100 to the maximal recorded response.

NFAT activation assay

Spleen and LN cells from control, CnB ΔTreg, or CD28 ΔTreg mice before onset of overt autoimmunity were kept on ice immediately upon harvest, during enrichment of Treg using the Miltenyi mouse Treg selection kit, and dead cell staining with Zombie Red (BioLegend). Some samples were stimulated with ionomycin (1 μg/ml; Sigma) for 10 min at 37˚C, whereas others were kept on ice to preserve their in situ NFAT activation state. All samples were allowed to adhere to poly-L-lysine–coated cover glasses for 5 min at 37˚C, then fixed in 4% PFA for 10 min and stained with anti-NFAT1 (D43B1; Cell Signaling), anti-NFAT2 (7A6; BioLegend), and anti-Foxp3 (FJK-16s; eBioscience) Abs. Primary Ab binding was revealed using Alexa Fluor 633–conjugated anti-rabbit IgG, Alexa Fluor 647–conjugated anti-mouse IgG Fab (Jackson Immunoresearch), and Alexa Fluor 488–conjugated anti-rat IgG (Invitrogen), respectively. Slides were mounted using ProLong antifade medium (Thermo Fisher) and analyzed on a Zeiss LSM510 confocal microscope. Nuclear localization of NFAT proteins was quantified as the

signaling index of individual cells (30), which has a value of 0 for full cytoplasmic localization and 1 for complete nuclear localization.

Treg apoptosis assay

Splenocytes and LN cells from CnB ΔTreg^{het}, CD28 ΔTreg^{het}, or Foxp3$^{YFP\text{-}Cre/wt}$ mice were assayed immediately after isolation or after 6 h of culture at 37˚C, to reveal Treg susceptibility to apoptosis, as described (3). Viability of CD4$^+$ YFP$^+$ CD62L^{hi} CD44^{low} cTreg was read out by Annexin V and 7-AAD staining, performed as per the manufacturer's instructions (BioLegend).

Isolation of lymphocytes from nonlymphoid tissues

Tumors, ear skin, lungs, liver, and colon were finely minced and processed with tissue-specific protocols as follows: tumor tissue was digested in RPMI 1640 5% FCS containing 1.5 mg/ml collagenase IV and 50 U/ml DNase I for 30 min; skin was digested in DMEM 2% FCS 10 mM HEPES containing 0.5 mg/ml hyaluronidase, 1.5 mg/ml collagenase IV, and 50 U/ml DNase I for 1 h; lungs were digested in DMEM 2% FCS 10 mM HEPES containing 0.5 mg/ml hyaluronidase, 1.5 mg/ml collagenase IV, and 50 U/ml DNase I for 20 min; and liver was digested in RPMI 1640 5% FCS supplemented with 1 mg/ml collagenase IV for 30 min. To isolate lymphocytes from the colon lamina propria, intraepithelial lymphocytes were eliminated by two 20 min washes in RPMI 1640 5% FCS 1.5 mM EDTA 1 mM DTT at 37˚C. After a brief wash in PBS to remove EDTA, the tissue fragments were incubated in RPMI 1640 5% FCS containing 1 mg/ml collagenase IV for 45 min. All digestions were performed at 37˚C under agitation, residual aggregates were mechanically disrupted, and cell suspensions were filtered before immunophenotyping.

Flow cytometric immunophenotyping

Dead cells were stained using the fixable viability dye Zombie Red according to the manufacturer's instructions. Chemokine receptors CCR4 (clone 2G12), CXCR3 (CXCR3-173), and CCR5 (HM-CCR5) were stained for 1 h at 37˚C in cell culture medium. Staining for CD4 (GK1.5), CD25 (PC61), CD44 (IM7), CD45 (30F11), CD62L (MEL14), and ICOS (C398.4A) was performed at 4˚C for 20 min. All these Abs were from BioLegend. To detect intracytoplasmic and intranuclear Ags, cells were fixed and permeabilized using the Mouse Regulatory T cell Staining Kit from eBioscience, and stained for Ki67 (16A8; BioLegend), CTLA-4 (UC10-4B9; BioLegend), GFP/YFP (Alexa Fluor 488–conjugated polyclonal rabbit IgG; Life Technologies), and Foxp3 (FJK-16s; eBioscience).

For some experiments, as indicated, blood-borne were distinguished from tissue-resident Treg by an i.v. injection of 3 μg CD45.2-PE mAb (clone 104) 3 min before euthanasia.

PCR to examine CnB locus rearrangement

DNA of Foxp3$^{YFP\text{-}Cre}$ or CnB ΔTreg mice was extracted either from tail tissue or from CD4$^+$ Foxp3$^+$ Treg sorted to >99% purity from LNs using the Arcturus PicoPure DNA extraction kit from Applied Biosystems. A fragment of the CnB locus containing the CnB open reading frame (and both flanking loxP sites in CnB ΔTreg) was amplified by PCR using the primers: 5′-CAATGCAGTCCGCTGTAGTTC-3′ and 5′-AGCCTCCACATACACAGATAC-3′.

Statistical analysis

For data passing the Kolmogorov–Smirnov normality test, experimental groups were compared through Student *t* test. Otherwise, Mann–Whitney *U* test was used.

Results

Treg require both calcineurin and CD28 to maintain immune homeostasis

A fraction of Treg in LNs continuously recognizes their cognate tissue-derived Ags (4, 31, 32), which is thought to enhance their suppressive function (8, 9) and to maintain immune homeostasis by extinguishing incipient autoimmune effector responses (33, 34). We sought to examine in this context the role of TCR- and calcineurin-dependent NFAT activation on the one hand, and of CD28-dependent complementation or amplification of TCR signals on the other hand. We therefore crossed Foxp3$^{YFP\text{-}Cre}$ knock-in mice (27) with animals in which both alleles either of the regulatory B subunit of calcineurin (CnB) (26) or of CD28 (14) genes were flanked by loxP sites to create Foxp3$^{YFP\text{-}Cre}$ × CnB$^{fl/fl}$ (henceforth "CnB ΔTreg") or Foxp3$^{YFP\text{-}Cre}$ × CD28$^{fl/fl}$ ("CD28 ΔTreg") mice. Because Foxp3 expression is initiated during the final steps of thymic Treg development (35), CnB or CD28 are efficiently deleted in mature Treg in these animals (Supplemental Fig. 1A) (14). CnB ΔTreg mice were born at Mendelian ratios and did not show macroscopic abnormalities until their fourth week of life, when they started to develop a hunched posture, scaly skin, crusted ears, and alopecia, and stopped thriving, whereas CD28 ΔTreg mice remained indistinguishable from littermates (Fig. 1A, 1B). CnB ΔTreg mice, but not CD28 ΔTreg mice, required euthanasia at a median age of 32 d because of a rapidly progressive wasting disease (Fig. 1C). In contrast to their normal appearance, CD28 ΔTreg mice already showed moderate splenomegaly and lymphadenopathy at 4 wk of age, but these signs were more prominent in CnB ΔTreg mice (Fig. 1D). Concomitantly, expansion of conventional CD8$^+$ and CD4$^+$ T cells with a CD44^{hi} CD62L^{neg} effector phenotype was already detectable at 2 wk of age in CnB ΔTreg mice, and more pronounced in these animals at 4 wk, when it became first detectable in CD28 ΔTreg mice (Fig. 1E, Supplemental Fig. 1B). Histological examination of nonlymphoid tissues of CnB ΔTreg mice revealed severe inflammatory infiltrates and associated pathological changes in the lungs, skin, and liver (Fig. 1F). Heart, kidney, adrenal glands, eye, and brain lacked infiltrates, whereas stomach and small and large intestines were only marginally affected (data not shown). By contrast, lungs of CD28 ΔTreg mice showed only focal inflammatory cell infiltrates and the majority of lung tissue remained unaffected. Skin and liver were marginally infiltrated (Fig. 1F), and all other organs appeared normal at this age (data not shown). Thus, whereas CD28 ΔTreg mice largely maintain immune homeostasis, and only later in life develop a skin-focused, nonlethal autoimmune disease (14, 15), CnB ΔTreg mice rapidly develop a lymphoproliferative inflammatory syndrome that, with regard to kinetics and organ distribution, closely resembles the scurfy phenotype in animals that either express a nonfunctional Foxp3 protein (36), in which Foxp3 is deleted (37), or in which Treg are ablated starting at birth (29).

Treg lacking calcineurin are suppressive, but proliferate poorly

Preceding and at the onset of overt disease in CnB ΔTreg mice at 4 wk of age, the frequency of Treg in LNs was only moderately reduced in CnB ΔTreg and CD28 ΔTreg mice, if at all (Fig. 2A), indicating that a Treg functional defect, not a defect in maintenance, causes lymphoproliferative disease in these animals. In contrast to LNs, we observed a clear and progressive reduction in Treg frequencies in spleens of both strains. This may result in part from preferential accumulation of the expanding populations of CD44^{hi} CD62L^{neg} conventional effector and effector memory T cells in spleens, including the splenic red pulp, as opposed to LNs (38), causing a relative decrease in Treg frequencies mostly in spleens. In addition, if splenic accumulation of conventional effector and effector memory T cells is in part based on their homing preferences, not local activation, they likely will produce less IL-2 to enable a concomitant local expansion of Treg to maintain their density (33). Thus, failed immune homeostasis in CnB ΔTreg and CD28 ΔTreg mice cannot be explained by Treg absence. However, when we examined the Treg compartment in SLOs for the proportion of CD44^{low} CD62L^{hi} cTreg and CD44^{hi} CD62L^{neg} eTreg, we found that eTreg were underrepresented in LNs and spleen of CnB ΔTreg mice, whereas the ratios of cTreg and eTreg were normal in CD28 ΔTreg mice (Fig. 2B). These observations suggested a role for calcineurin activity in the

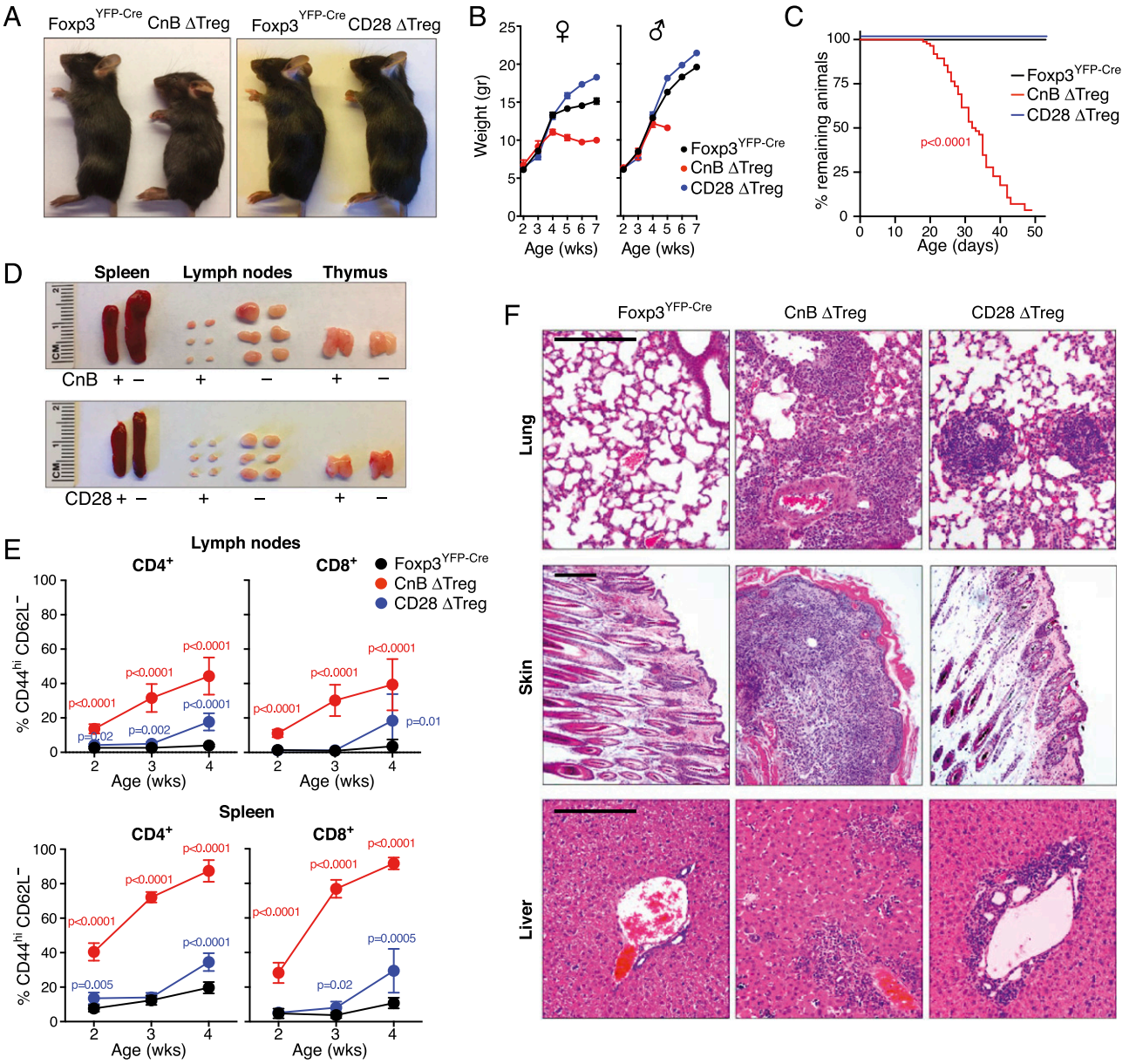

FIGURE 1. Treg depend on calcineurin, but less so on CD28 to maintain immune homeostasis. (**A**) Four-week-old Foxp3$^{YFP\text{-}Cre}$, CnB ΔTreg, and CD28 ΔTreg mice. (**B**) Growth curves of Foxp3$^{YFP\text{-}Cre}$ (18 male, 13 female), CnB ΔTreg (6 male, 6 female), and CD28 ΔTreg (26 male, 10 female) mice. (**C**) Survival of Foxp3$^{YFP\text{-}Cre}$ ($n = 28$), CnB ΔTreg ($n = 89$), and CD28 ΔTreg mice ($n = 10$). Mice were euthanized when moribund. The p value was calculated by Mantel–Cox test. (**D**) Splenomegaly and lymphadenopathy in 4-wk-old CnB ΔTreg and CD28 ΔTreg mice. (**E**) Frequencies of CD44^{hi} CD62L^{neg} conventional (Foxp3$^-$) CD4$^+$ and CD8$^+$ T cells in the LNs and spleen of 2–4-wk-old mice. Foxp3$^{YFP\text{-}Cre}$: $n = 6$–10; CnB ΔTreg: $n = 3$–5; CD28 ΔTreg: $n = 5$ per time point. Mean ± SEM are depicted. The p values were calculated through Student t test. (**F**) H&E-stained sections of lung, skin, and liver from 4-wk-old mice. Scale bar, 200 μm.

TCR-dependent formation of eTreg, which may contribute to failed immune homeostasis in CnB ΔTreg mice despite the presence of Foxp3$^+$ Treg.

To directly compare the function of calcineurin- and CD28-deficient cTreg as well as eTreg, we examined their in vitro suppressive activity separately. In order to avoid the potentially confounding effects of overt or subclinical systemic inflammation in CnB ΔTreg and CD28 ΔTreg mice on the function of Treg, we generated female Foxp3$^{YFP\text{-}Cre/wt}$ × CnB$^{fl/fl}$ ("CnB ΔTreg^{het}") and Foxp3$^{YFP\text{-}Cre/wt}$ × CD28$^{fl/fl}$ ("CD28 ΔTreg^{het}") animals. Because the Foxp3 locus is located on the X chromosome, random X inactivation will predictably lead to expression of YFP-Cre and deletion of CnB or CD28 in only half of all Treg (YFP$^+$), whereas the other half (YFP$^-$) does not delete these genes and maintains immune homeostasis (Fig. 2C). These mice had normal lifespans (Supplemental Fig. 2A) and remained healthy with no signs of conventional effector T cell expansion (Supplemental Fig. 2B) or lymphocytic tissue infiltration as observed in CnB ΔTreg and CD28 ΔTreg mice (Supplemental Fig. 2C). However, we noted that consistently <50% of Treg expressed YFP-Cre in lymphoid tissues even in the absence of any floxed allele (Supplemental Fig. 2D), potentially reflecting toxic effects of the Cre recombinase on cryptic loxP sites in the mouse genome (39). To control for this possibly confounding effect, we used YFP-Cre–expressing Treg from Foxp3$^{YFP\text{-}Cre/wt}$ mice as controls ("WT Treg").

When we cocultured purified YFP$^+$ cTreg from CnB ΔTreg^{het}, CD28 ΔTreg^{het}, or Foxp3$^{YFP\text{-}Cre/wt}$ mice for 3 d with CD4$^+$ responder T cells and T cell–depleted splenocytes in the presence of

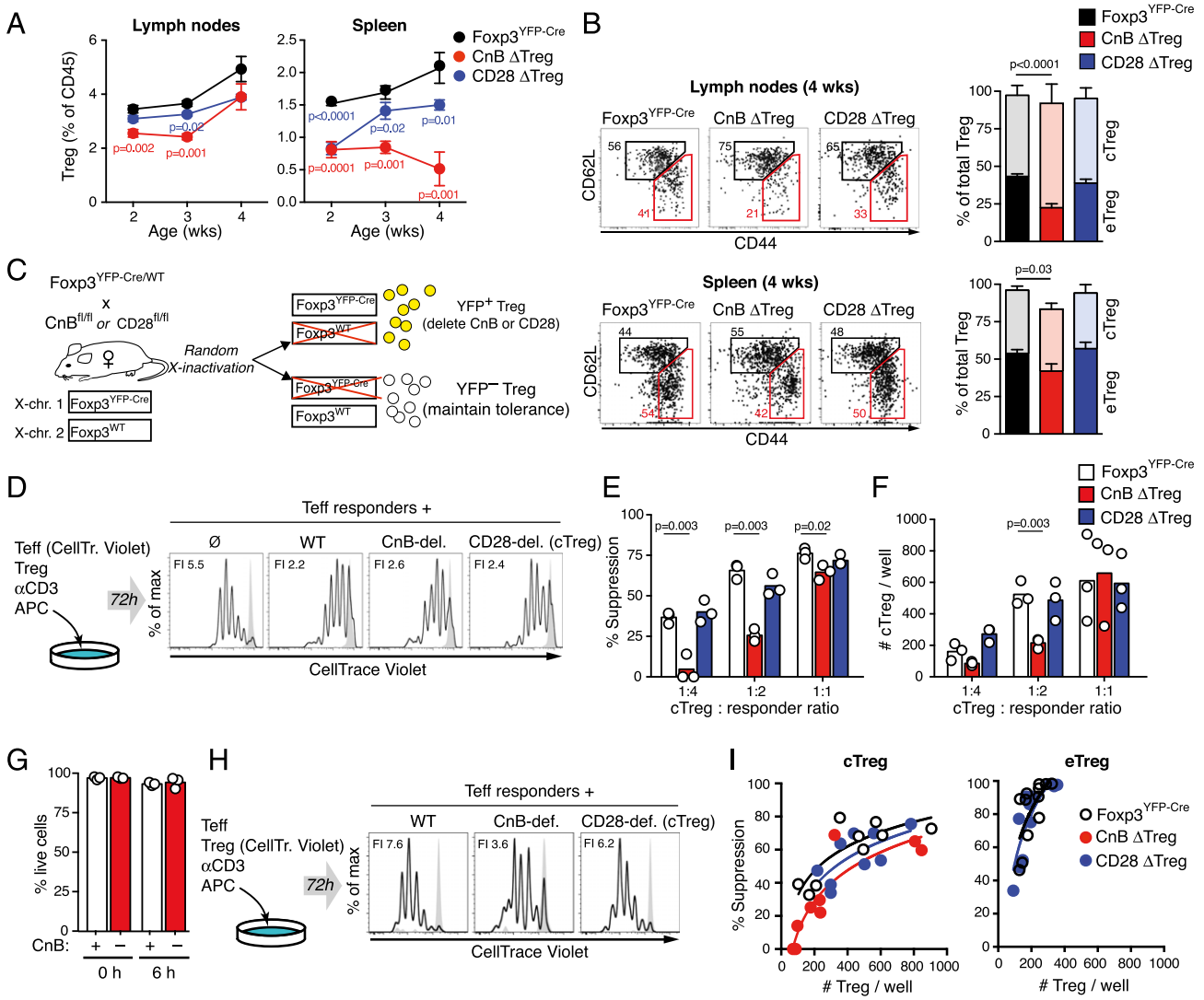

FIGURE 2. CnB- or CD28-deficient Treg retain suppressive activity in vitro. (**A**) Frequency of Treg in skin-draining LNs and spleen at the indicated ages. Mean ± SEM are shown. Foxp3$^{YFP\text{-}Cre}$: n = 6–7; CnB ΔTreg: n = 3–5; CD28 ΔTreg: n = 4–5 per time point. The p values were calculated by Student t test. (**B**) Proportions of CD44^{low} CD62L^{hi} cTreg and CD44^{hi} CD62L^{neg} eTreg in LNs and spleen of Foxp3$^{YFP\text{-}Cre}$ control (n = 10), CnB ΔTreg (n = 8), and CD28 ΔTreg (n = 5) mice. Mean and SEM are shown. The p value was calculated through Student t test. (**C**) Female heterozygous Foxp3$^{YFP\text{-}Cre}$ mice crossed to CnB$^{fl/fl}$ or CD28$^{fl/fl}$ animals produce YFP^{+} Treg that delete CnB or CD28 and YFP^{-} Treg that maintain immune homeostasis. (**D**) In vitro–suppressive activity of purified cTreg lacking CnB or CD28. Histograms show proliferation of CD4^{+} responder T cells (Teff) cocultured for 3 d with APCs and anti-CD3 Abs in absence or in presence of WT, CnB-deficient, or CD28-deficient cTreg. Gray histograms represent unstimulated responder cells. FI = fold increase in number of responder T cells. (**E**) Rate of suppression at increasing cTreg:responder ratios. One experiment representative of two is shown. The p values were calculated by Student t test. (**F**) Absolute numbers of Treg recovered from each well at the end of the 3-d culture period. Results are representative of two experiments. The p values were calculated by Student t test. (**G**) Proportion of live (Annexin V^{-} 7-AAD^{-}) cTreg before or after 6 h of culture in absence of IL-2. Graphs show three technical replicates and their mean. One experiment out of two is shown. (**H**) Proliferation of Treg over 72 h of coculture with APCs, anti-CD3 Abs, and conventional T cells. Gray histograms show unstimulated Treg. FI = cTreg fold increase. One experiment representative of two is shown. (**I**) cTreg (left) and eTreg (right)-mediated suppressive activity as a function of the corresponding number of Treg in individual wells at the end of the coculture. Numbers of CnB-deficient eTreg available were insufficient for analysis. Lines represent the semilog best fits. Data are representative of two independent experiments.

anti-CD3 Abs, we found that CnB-deficient cTreg suppressed responder cell proliferation at almost normal levels, and defective suppression only became evident at low cTreg:responder ratios (Fig. 2D, 2E). Of note, reduced suppressive activity of CnB-deficient Treg correlated with lower Treg numbers retrieved at the end of the 3-d assay (Fig. 2F). In contrast, CD28-deficient cTreg functioned normally and accumulated similarly to controls (Fig. 2E, 2F). Lower numbers of CnB-deficient Treg did not appear to result from enhanced apoptosis (Fig. 2G), but mostly from a pronounced proliferation defect (Fig. 2H). This suggested that poor proliferation and accumulation of CnB-deficient Treg may primarily account for their reduced in vitro–suppressive activity. Therefore, to determine the suppressive capacity of CnB-deficient and CD28-deficient cTreg on a per cell basis, we quantified their suppression of responder cell proliferation as a function of their numbers at the end of the assay. By this measure, both CnB-deficient and CD28-deficient cTreg showed near-normal suppressive activity, as they allowed only ~20 and ~10% more responder T cell proliferation than control cells, respectively (Fig. 2I). eTreg were more potent suppressors than cTreg on a per cell basis, as expected, and their function was not detectably impaired in absence of CD28 (Fig. 2I). CnB-deficient eTreg, because of their paucity in

CnB ΔTreg^{het} mice, could not be isolated in sufficient numbers for functional testing. Together, these observations reveal no or only minor defects in cTreg lacking CnB or CD28. Because prior studies correlated similarly mild in vitro–suppressive defects in Treg with no or only mild autoimmune phenotypes (40, 41), we hypothesized that failed immune homeostasis, and especially the scurfy phenotype in CnB ΔTreg mice, may result mostly from a reduced capacity of CnB- or CD28-deficient eTreg to migrate to and persist in nonlymphoid tissues.

Lack of CD28 reduces and lack of CnB abrogates Treg accumulation in nonlymphoid tissues

In contrast to cTreg, which primarily express the chemokine receptors CCR7 and CXCR4, whose ligands are expressed in lymphoid tissues, eTreg are responsive to chemokines that guide their migration to nonlymphoid tissues (2, 11, 42, 43). For instance, genetic deletion of CCR4 in Treg strongly impairs their capacity to migrate into skin and lung, and leads to severe skin and pulmonary inflammation (13). This suggests that immune homeostasis not only requires Treg activity in SLOs, where immune responses are induced, but also in nonlymphoid tissues. We therefore hypothesized that impaired eTreg differentiation in absence of CnB or CD28 may account for reduced accumulation in nonlymphoid tissues, causing the widespread tissue inflammation described above. To test this hypothesis, we examined female CnB ΔTreg^{het} and CD28 ΔTreg^{het} mice, where tissue distribution of YFP$^+$ Treg lacking either CnB or CD28 can be studied in a noninflammatory context (see Fig. 2C, Supplemental Fig. 2). Here, the frequency of YFP$^+$ Treg was decreased in LNs of CnB ΔTreg^{het} relative to control animals (Fig. 3A), suggesting that the normal Treg numbers in LNs of CnB ΔTreg mice are sustained in part by inflammation. Moreover, specifically the proportion of CD44^{hi} eTreg was diminished in these animals (Fig. 3B, Supplemental Fig. 2E). To investigate eTreg formation in more detail, we measured the expression of the Treg activation markers ICOS and CTLA-4 and of the cell cycle entry marker Ki67. Basal expression of ICOS and CTLA-4 in cTreg was unchanged. However, their elevated expression in WT eTreg was diminished by nearly 10-fold in the absence of CnB, and ∼2-fold in the absence of CD28. Ki67 was equally reduced in both cases (Fig. 3C). Furthermore, CXCR3, CCR4, and CCR5, chemokine receptors that are expressed in a fraction of CD44^{hi} eTreg and confer tropism for nonlymphoid tissues, were undetectable in Treg lacking CnB, but only reduced in those lacking CD28 (Fig. 3C), suggesting a critical role for CnB-driven NFAT activity in inducing expression of eTreg-associated chemokine genes. To examine this further, we parsed a published NFAT1 chromatin immunoprecipitation sequencing data set obtained from CD8$^+$ T cells (44) to determine the distance from the transcription start sites (TSSs) of chemokine receptor genes to the closest NFAT1 binding sites. In comparison with all other genes in this data set, or a collection of control genes implicated in stem cell function, TSS-NFAT1 binding site distances for chemokine receptor genes were very short, with 80% being $<$10 kb (compared with ∼40% of the stem cell genes and 36% for all genes), and 56% being $<$2 kb (compared with 25 and 20% for stem cell–related and all genes) (Supplemental Fig. 3A). Specifically, CCR4, CXCR3, and CCR5 had NFAT1 binding sites within 72, 1763, and 4709 bp of their TSSs (Supplemental Fig. 3). This suggests that the CnB/NFAT axis directly regulates chemokine receptor gene expression in T cells, and that CnB-deficient Treg fail to induce CXCR3, CCR4, and CCR5 at least in part because of impaired transactivation of these genes by NFAT proteins. Treg that lacked costimulation via CD28 also expressed these chemokine receptors less frequently, but those that did, expressed them at similar levels as control Treg (Fig. 3C).

Impaired eTreg formation predicts reduced Treg accumulation in nonlymphoid tissues. Indeed, in all nonlymphoid tissues studied, including those that are most severely inflamed in CnB ΔTreg mice, we noted that CnB-deficient YFP$^+$ Treg were essentially absent (Fig. 3D). In contrast, the reduction of Treg lacking CD28 was milder and more variable, and most pronounced in skin, the tissue that is most affected by the inflammatory disease that CD28 ΔTreg mice develop later in life (14, 15). These findings suggest a scenario whereby TCR-driven CnB activity is critical and CD28 costimulation optimizes the formation of eTreg whose migration to and survival in nonlymphoid tissues is required for immune homeostasis.

CnB is essential for the differentiation of tumor-homing eTreg

The effects of CnB- or CD28-deletion on the ability of Treg to populate nonlymphoid sites may also restrict their migration and persistence in tumor tissue, and thereby limit their ability to establish local tumor tolerance. To test this hypothesis, and also to examine the role of CnB in enabling the formation of eTreg and their trafficking into a newly forming immune effector site, we implanted female CnB ΔTreg^{het} mice with fast-growing MCA-205 mesenchymal tumors. Eleven days after tumor implantation the frequency of YFP$^+$ Treg in tdLNs of control and CnB ΔTreg^{het} mice was comparable (Fig. 4A). However, CnB-deficient Treg were absent from tumor tissue, suggesting that without calcineurin activity, Treg cannot acquire the functions that enable them to enter and survive in tumor tissue. Similar to Treg in which TCRs are deleted (8, 9), we found a small but consistent reduction in Foxp3 expression in CnB-deficient Treg in tdLNs (Fig. 4B), which possibly reflects the reported role of CnB-dependent NFAT activity on CNS2 to stabilize Foxp3 expression (45). We also noted that although essentially all CnB-sufficient Treg in tumor tissue and more than 50% in tdLNs were CD44^{hi} CD62L^{neg} eTreg, $<$20% of CnB-deficient Treg in tdLNs showed this phenotype, and those that did had only partially downregulated CD62L (Fig. 4C). Hence, lack of CnB limits, but does not abolish, CD44 up- and CD62L downregulation, cardinal features of T cell activation.

Because migration of Treg into tumor tissue likely requires appropriate trafficking receptors, we analyzed expression of chemokine receptors CXCR3, CCR4, and CCR5, which have previously been implicated in Treg accumulation in tumor tissue (46–48). All three receptors were expressed by varying fractions of WT CD44^{hi} eTreg in tdLNs (Fig. 4D), and the majority of Treg in tumor tissue expressed these receptors, demonstrating that their expression correlated with the ability of Treg to accumulate in tumors. In contrast, CnB-deficient Treg completely failed to express any of these chemokine receptors (Fig. 4D). Hence, failure to induce expression of appropriate trafficking molecules is one likely reason for their inability to enter tumor tissue.

In addition to trafficking receptors, eTreg express elevated levels of CTLA-4, required for their suppressive function (49), and ICOS, which has been suggested to promote their survival (3). Strikingly, the rare CD44^{hi} CnB-deficient Treg in tdLNs completely failed to induce expression of ICOS and CTLA-4 above baseline levels found in cTreg, and their proliferation was strongly impaired (Fig. 4E). In contrast, all tumor-infiltrating WT Treg expressed high levels of ICOS, CTLA, and the cell cycle entry marker Ki67, suggesting that these features are either correlated with or a prerequisite for accumulation in tumor tissue.

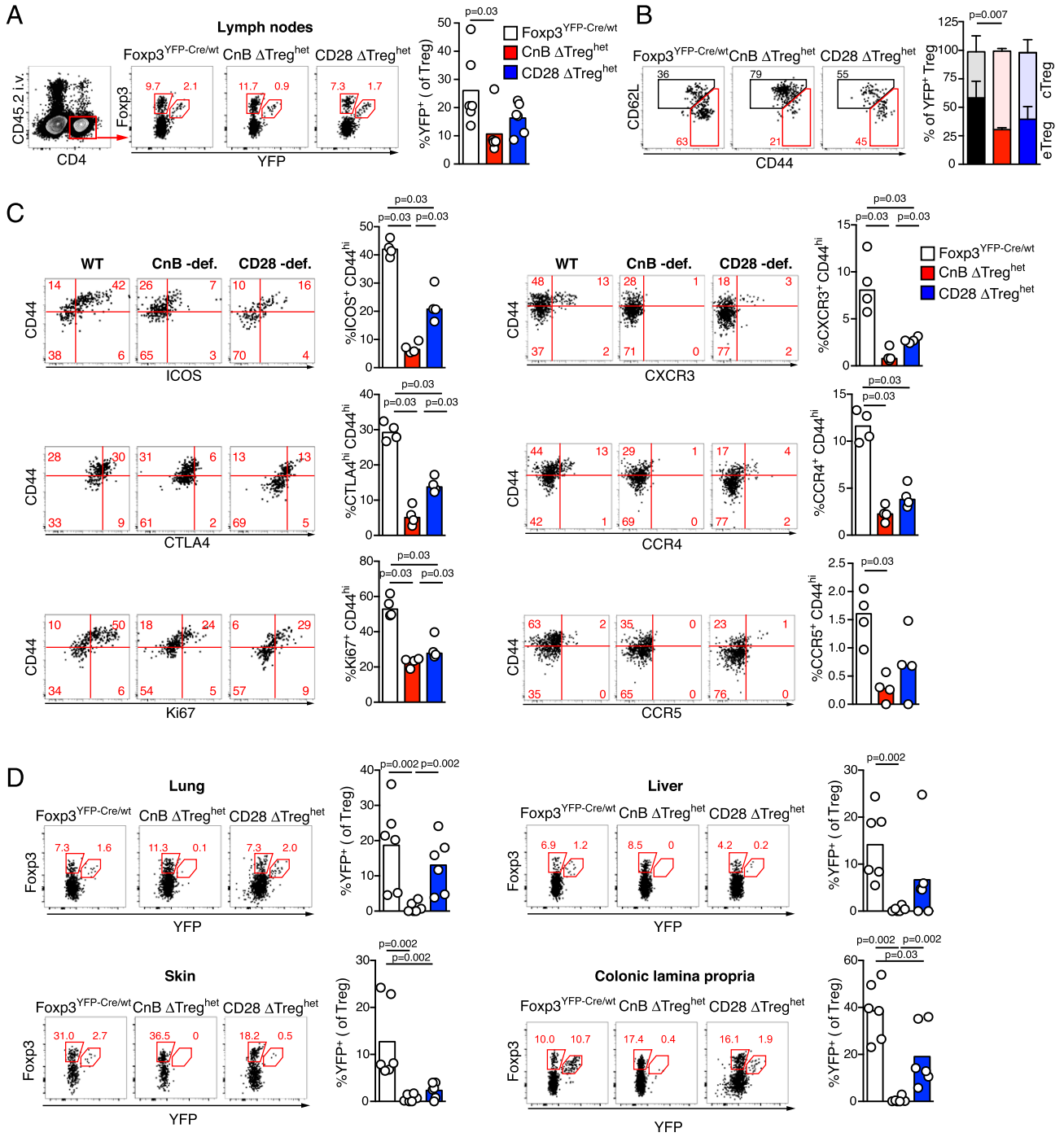

FIGURE 3. Impaired accumulation of CnB- or CD28-deficient Treg in nonlymphoid tissues. (**A**) Gating and frequency of extravascular YFP$^+$ Treg in LNs of female Foxp3$^{YFP\text{-}Cre/wt}$, CnB ΔTreg^{het}, or CD28 ΔTreg^{het} mice. Bars represent medians. The p values were calculated by Mann–Whitney U test. (**B**) Frequencies of CD44^{low} CD62L^{hi} cTreg and CD44^{hi} CD62L^{neg} eTreg among total YFP$^+$ Treg in LN. Mean and SEM are depicted. The p values were calculated by Student t test. (**C**) Expression of ICOS, CTLA-4, Ki67, CXCR3, CCR4, and CCR5 on YFP$^+$ Treg in the LNs of the indicated mice. Bars represent medians. The p values were calculated by Mann–Whitney U test. (**D**) Frequency of YFP$^+$ Treg in the indicated tissues. Bars represent medians. The p values were calculated using Mann–Whitney U test. In (A) and (D), data are pooled from two independent experiments, $n = 6$ per group. In (B) and (C), one experiment ($n = 4$ per group) representative of three is shown.

These observations suggest, but do not formally prove that CD44^{low} cTreg convert into CD44^{hi} eTreg during tumor challenge upon TCR-dependent activation in tdLNs. To more stringently test this model, we seeded mice with clonal populations of TCR-transgenic cTreg specific for the model Ag influenza HA (7, 30) and tracked their proliferation and concomitant differentiation into eTreg, as well as their accumulation in tumors expressing HA. We found that cTreg upregulated CCR4, CCR5, and CXCR3, whereas downregulating CCR7 (Supplemental Fig. 4A), and also upregulated CTLA-4 and ICOS (Supplemental Fig. 4B) during Ag-driven clonal expansion in tdLN. Similarly to polyclonal Treg, only cells that had undergone extensive proliferation and expressed the most CTLA-4 and ICOS accumulated in tumor tissue. Thus, TCR signaling and, more specifically, CnB activation play a cell-intrinsic and nonredundant role in driving cTreg to eTreg differentiation in tdLNs, and their subsequent accumulation within tumors.

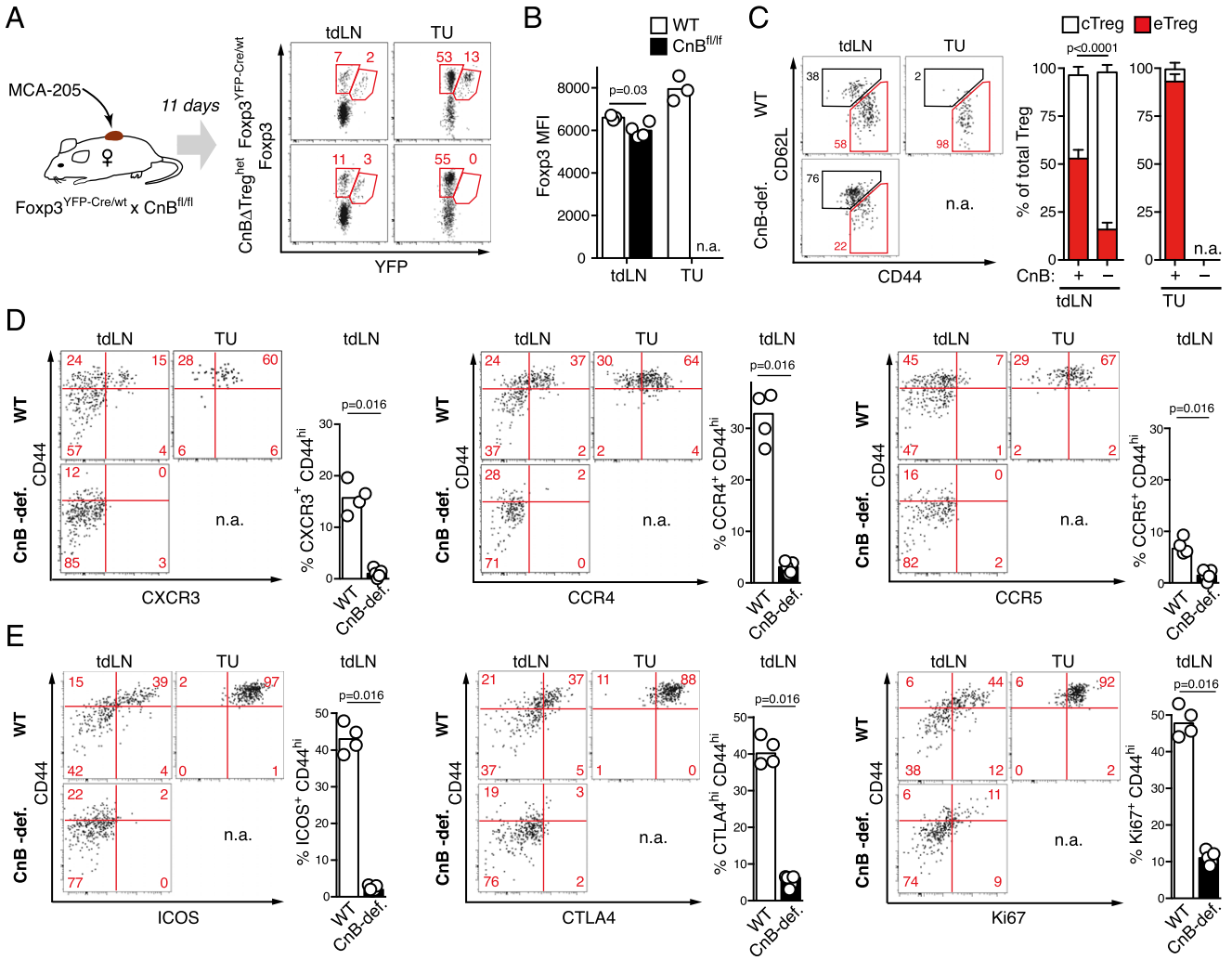

FIGURE 4. CnB-deficient Treg fail to differentiate into tumor-homing eTreg. (**A**) Frequencies of YFP$^+$ Foxp3$^+$ Treg among CD4$^+$ T cells in tdLNs and tumor tissue 11 d after implantation of MCA-205 tumors into Foxp3$^{YFP\text{-}Cre/wt}$ or CnB ΔTreg^{het} mice. One representative result of 14 mice in four separate experiments is shown. (**B**) Foxp3 expression in CnB-sufficient and CnB-deficient YFP$^+$ Treg in tdLNs and tumor tissue. One experiment representative of four is shown. The *p* values were calculated by Student *t* test. (**C**) Frequencies of CD44^{low} CD62L^{hi} cTreg and CD44^{hi} CD62L^{neg} eTreg among total YFP$^+$ Treg in tdLNs and tumors in CnB ΔTreg^{het} and Foxp3$^{YFP\text{-}Cre/wt}$ control mice. Mean and SEM of one experiment (n = 4–5 per group) representative of four are shown. The *p* values were calculated by Student *t* test. (**D**) CXCR3, CCR4, and CCR5 expression in YFP$^+$ CD44^{low} cTreg and CD44^{hi} eTreg in tdLNs as well as tumor tissue in CnB ΔTreg^{het} (CnB-def.) and Foxp3$^{YFP\text{-}Cre/wt}$ (WT) control mice 11 d after tumor implantation. (**E**) ICOS, CTLA-4, and Ki67 expression in YFP$^+$ CD44^{low} cTreg and CD44^{hi} eTreg in the indicated tissues of CnB ΔTreg^{het} (CnB-def.) and Foxp3$^{YFP\text{-}Cre/wt}$ (WT) control mice. In both (D) and (E) quantification of one experiment (n = 4–5) out of three performed is shown. Bars represent medians. The *p* values were calculated by Mann–Whitney *U* test.

NFAT proteins are the main effectors of calcineurin activity in Treg

In conventional T cells, calcineurin is essential for TCR-mediated activation and nuclear accumulation of the T cell–expressed NFAT proteins NFAT1, NFAT2, and NFAT4. However, recent reports have questioned the generality of this mechanism by describing a pathway of NFAT activation through IL-7 in thymocytes (50), as well as constitutive, TCR- and calcineurin-independent NFAT activity in Treg (21–25). To examine the mechanism of NFAT activation in Treg in SLOs, we purified Treg under conditions optimized to preserve their in situ NFAT activation state and examined subcellular localization of NFAT1 and NFAT2. Both proteins were nuclear in a sizeable fraction of WT Treg. In contrast, NFAT1 and NFAT2 proteins were cytoplasmic in essentially all CnB-deficient Treg (Fig. 5A, 5B). Treatment with the Ca^{2+} ionophore ionomycin triggered further nuclear translocation of NFAT1 and 2 in the majority of WT Treg, but was completely ineffective in CnB-deficient Treg (Fig. 5A, 5B). Similar observations were made under stimulation of Treg with Con A, which crosslinks the TCR and various costimulatory receptors (data not shown). Hence, a fraction of Treg in lymphoid tissues receives signals that activate NFAT1 and NFAT2 in the steady state, but this activity, as well as additional TCR and Ca^{2+}-induced activity, is fully dependent on calcineurin.

In addition to NFAT proteins, calcineurin might help to activate other signaling activities, such as the NF-κB pathway via the CARMA1/Bcl10/MALT1 complex (51). To investigate these functions of calcineurin in Treg, we conducted phosphoprotein analysis by flow cytometry on YFP$^+$ Treg from CnB ΔTreg^{het} and Foxp3$^{YFP\text{-}Cre/wt}$ mice. Upon TCR stimulation of CnB-deficient cells, we observed no defect in Ras/ERK activation, no defect in mTORC1 activity as reflected by S6 phosphorylation, and slightly enhanced, but not diminished, NF-κB activity, as reflected by degradation of IκB (Fig. 5C, 5D). Similar results were obtained using suboptimal doses of anti-CD3 stimulation, ruling out a

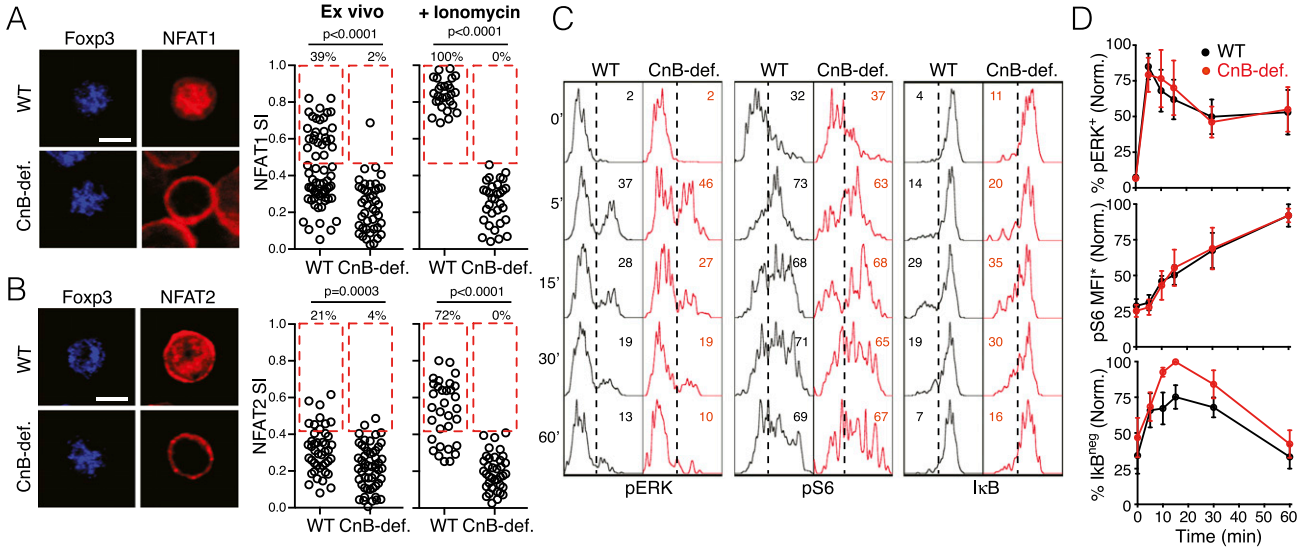

FIGURE 5. NFAT proteins are the main effectors of CnB activity in Treg. (**A** and **B**) CD4$^+$ CD25$^+$ T cells were purified from LNs and spleens of CnB ΔTreg and Foxp3$^{YFP\text{-}Cre}$ control mice and stained for Foxp3 and either NFAT1 (A) or NFAT2 (B) immediately (ex vivo) or after stimulation with ionomycin (+ionomycin). The fraction of nuclear (colocalized with Foxp3) among total cellular NFAT is quantified as the NFAT Signaling Index (SI). Red rectangles highlight cells with SIs above background, whose frequency is shown as percentage. Scale bar, 5 μm. One experiment out of three (A) or two (B) is shown. The *p* values were calculated by Mann–Whitney *U* test. (**C**) Time-course of ERK and S6 phosphorylation and IκB downregulation in YFP$^+$ WT Treg from CnB ΔTreg^{het} or Foxp3$^{YFP\text{-}Cre/wt}$ mice after anti-CD3/CD28 stimulation. Histograms are representative of four independent experiments. Gates are set based on fluorescence recorded on unstimulated CD4$^+$ conventional effector T cells with comparable physical characteristics to Treg. Values indicate frequencies of pERK$^+$, pS6$^+$, and IκB^{neg} cells. (**D**) Comparison of ERK and S6 phosphorylation and IκB downregulation in YFP$^+$ Treg from CnB ΔTreg^{het} and Foxp3$^{YFP\text{-}Cre/wt}$ control mice. Mean ± SEM of normalized mean values from four independent experiments, each performed in triplicate, are shown. pS6 MFI* indicates frequency of pS6$^+$ cells multiplied with their MFI.

masking effect of excessive TCR stimulation at high anti-CD3 doses, as well as with pharmacological stimulation by PMA and ionomycin (data not shown). Hence, activation of NFAT1 and 2 is fully dependent on calcineurin activity, and NFAT activation is the primary effector pathway in Treg, suggesting that the failure of CnB-deficient Treg to form eTreg and maintain immune homeostasis mainly results from lack of NFAT activity.

CD28 costimulation optimizes the formation of tumor-homing eTreg independently of NFAT activation

In light of the critical need for TCR-driven NFAT activation via calcineurin for induction of the eTreg trafficking program and elevated suppressive function, we asked whether costimulation via CD28 had an augmenting and qualitatively similar or a qualitatively distinct role in this process. CD28 is critical for the formation of conventional effector T cells and has been described as a general amplifier of TCR-induced signaling pathways, including the activation of NFAT proteins (52, 53), but is also critical for triggering distinct activities, including maximal NF-κB activation (54, 55). To first determine if CD28 synergizes with calcineurin in NFAT activation in Treg, we examined YFP$^+$ Treg from SLOs of CD28 ΔTreg^{het} mice. In situ activation of NFAT1 and 2 and their ionomycin-triggered nuclear translocation were normal in CD28-deficient Treg (Fig. 6A, data not shown). In contrast, and consistent with previous analyses on conventional T cells (54, 55), we found CD28 to be critical for TCR-dependent NF-κB activation in mature Treg (Fig. 6B). Therefore, in Treg, CD28 costimulation regulates TCR-dependent signaling activities distinct from those that depend on calcineurin (Fig. 5D).

To determine the role of CD28 in the formation of eTreg that can infiltrate tumor tissue, we compared their distribution in CD28 ΔTreg^{het} and Foxp3$^{YFP\text{-}Cre/wt}$ control mice implanted with MCA-205 tumors. In contrast to the normal frequency of eTreg in LNs of CD28 ΔTreg or CD28 ΔTreg^{het} mice (Figs. 2B, 3B), we observed a 50% decrease in CD28-deficient eTreg in tdLNs of CD28 ΔTreg^{het} mice (Fig. 6C). This difference may result from the fact that in CD28 ΔTreg^{het} mice, CD28-deficient Treg have to compete with CD28-sufficient Treg for potentially limiting resources, for example, ICOS ligands (3), which restrict their survival as eTreg. However, in contrast to CnB-deficient Treg, CD28-deficient eTreg migrated to tumor tissue (Fig. 6C), albeit at a frequency of <10% of normal (data not shown). Although fewer CD28-deficient Treg expressed CXCR3, CCR4, and CCR5 in tdLNs, those that did, expressed these receptors at the same levels as WT eTreg (Fig. 6D). Similar observations were made for CTLA-4 and ICOS: CD28-deficient eTreg expressing these proteins were less abundant, but expressed them and proliferated at the same levels as WT eTreg (Fig. 6E).

In line with a selection of Treg responsive to inflammatory chemokines for tumor entry, the majority of CD28-deficient Treg in tumor tissue expressed CXCR3, CCR4, and CCR5 (Fig. 6F). CCR5 expression was slightly reduced in tumor-infiltrating Treg lacking CD28, suggesting that this receptor is less important for entry or local persistence than CXCR3, which was normal, or CCR4, which was slightly elevated (Fig. 6F).

Interestingly, in contrast to tdLN, eTreg expression of ICOS and, more variably, CTLA-4 was reduced, indicating that CD28 costimulation is necessary to sustain optimal Treg function at effector sites (Fig. 6G). Thus, although CnB-deficient Treg are unable to acquire to any degree the state of elevated functional activity and trafficking capabilities of eTreg, CD28-deficient Treg remain capable of both and migrate to tumor tissue. Here they accumulate at reduced frequency and in a partially diminished state of activation.

Both calcineurin- and CD28-deficient Treg are defective in promoting tumor tolerance

Global ablation of Treg in mouse models enhances immunological control of tumors in both prophylactic and therapeutic settings. We

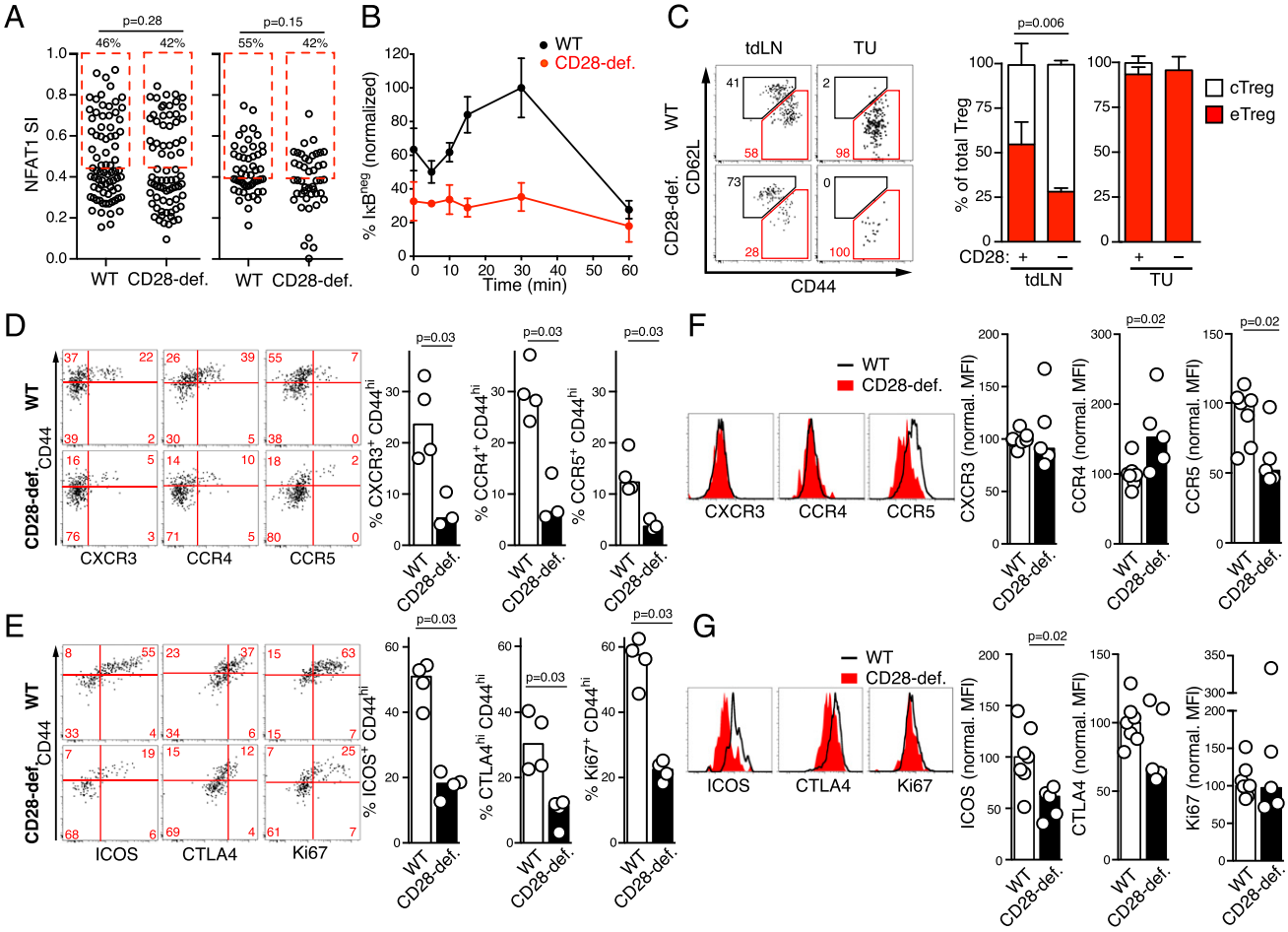

FIGURE 6. CD28 optimizes the differentiation of tumor-infiltrating eTreg. (**A**) Ex vivo analysis of NFAT1 and NFAT2 nuclear localization in control or CD28-deficient Foxp3^{+} Treg immediately upon isolation from LNs and spleen of CD28 ΔTreg or Foxp3$^{YFP\text{-}Cre}$ control mice and processed as described for Fig. 5A. One experiment out of two is shown. The *p* values were calculated by Mann–Whitney *U* test. (**B**) Analysis of IκB downregulation in YFP^{+} Treg from CD28 ΔTreg^{het} and Foxp3$^{YFP\text{-}Cre/wt}$ control mice. Mean ± SD of normalized average of triplicate measures are shown. One experiment representative of two is shown. (**C**) Frequencies of CD44^{low} CD62L^{hi} cTreg and CD44^{hi} CD62L^{neg} eTreg among total YFP^{+} Treg in tdLNs in CD28 ΔTreg^{het} or Foxp3$^{YFP\text{-}Cre/wt}$ control mice. Mean and SEM of one experiment (four mice per group) out of three are shown. (**D** and **E**) Expression of CXCR3, CCR4, and CCR5 (D) and ICOS, CTLA-4, and Ki67 (E) in YFP^{+} Treg in tdLNs of CD28 ΔTreg^{het} (CD28-def.) and Foxp3$^{YFP\text{-}Cre/wt}$ control mice (WT) 11 d after MCA-205 tumor implantation. In both (D) and (E) quantification of one experiment (n = 3–4) representative of three performed is shown. Bars represent medians. The *p* values were calculated by Mann–Whitney *U* test. (**F** and **G**) Expression of CXCR3, CCR4, and CCR5 (F) and ICOS, CTLA-4, and Ki67 expression (G) in tumor tissue of CD28 ΔTreg^{het} (CD28-def.) and Foxp3$^{YFP\text{-}Cre/wt}$ control (WT) mice 11 d after MCA-205 tumor implantation. Data are pooled from three independent experiments (n = 5–7). MFIs were normalized to the average MFI of WT Treg within each experiment. The *p* values were calculated by Mann–Whitney *U* test.

wanted to explore the effect specifically of preventing or reducing eTreg formation on tumor tolerance. Although meaningful tumor growth studies in CnB ΔTreg mice are not possible because of their short life span and severe inflammatory disease, we first examined the importance of CD28 costimulation for the ability of Treg to control antitumor immunity. When we implanted MCA-205 tumors into homozygous CD28 ΔTreg mice, we observed a significant deceleration of tumor growth compared with control animals, indicating enhanced antitumor immunity (Fig. 7A). Interestingly, the accumulation of CD28-deficient Treg in tumor tissue was less impaired (2–3-fold) in this setting than in CD28 ΔTreg^{het} mice (15–20-fold), where CD28-deficient and CD28-sufficient Treg potentially compete for resources (Fig. 7B, 7C). When we implanted the less aggressive colon carcinoma line MC38 into CD28 ΔTreg mice, tumor control was even more pronounced and two out of four animals rejected their tumors (Fig. 7D), suggesting that costimulation of Treg via CD28 is critical for tumor tolerance.

Although CD28 ΔTreg mice appear healthy, their latent lymphoproliferative disease may still confound tumor growth studies. To address this caveat, and also to enable comparative studies of animals with CD28- and CnB-deficient Treg, we devised two different strategies either to acutely delete CnB or CD28 in Treg, or to remove CnB- or CD28-sufficient Treg. First, we crossed CnB$^{fl/fl}$ and CD28$^{fl/fl}$ to Foxp3^{CreERT2} mice (28) to create CnB ΔTreg^{ind} and CD28 ΔTreg^{ind} mice, in which Cre activity is induced and CnB or CD28 genes are deleted in Treg only upon tamoxifen treatment. When we implanted MC38 carcinomas into these animals and initiated tamoxifen treatment 4 d later, both strains exerted partial control over tumor growth, but this control was more pronounced in CnB ΔTreg^{ind} mice (Fig. 7E). However, this approach is likely limited by incomplete deletion of floxed genes (8). Therefore, we devised a second approach and created mixed bone marrow chimeras from either CnB ΔTreg or CD28 ΔTreg together with Foxp3^{DTR} bone marrow cells. In these animals, Foxp3^{DTR} Treg maintain immune tolerance, but can be

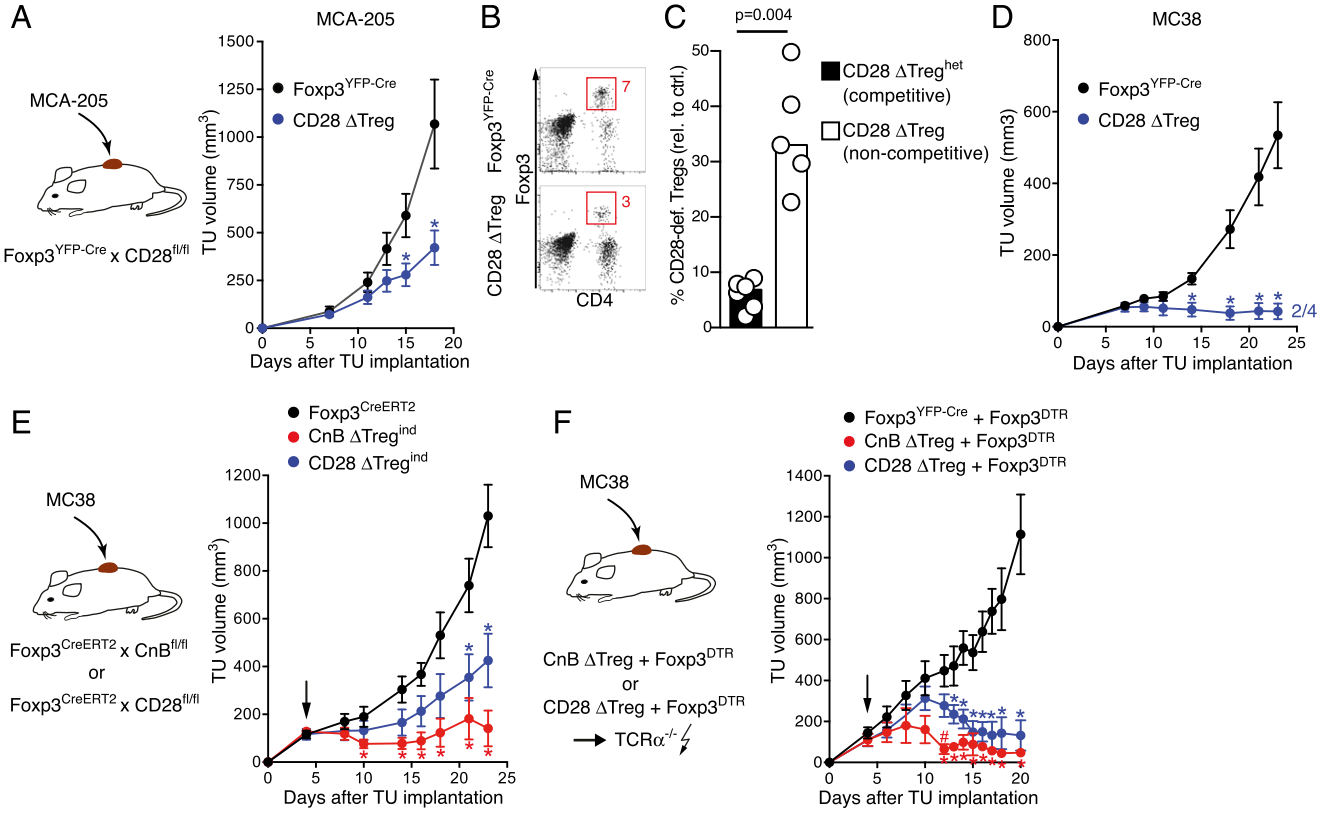

FIGURE 7. CnB-deficient Treg are more strongly impaired in maintaining tumor tolerance than CD28-deficient Treg. (**A**) Growth rates of s.c. MCA-205 tumors in CD28 ΔTreg ($n = 3$) or Foxp3$^{YFP\text{-}Cre}$ control mice ($n = 3$). Mean ± SEM for one experiment of two are shown. (**B**) Frequency of Foxp3$^+$ Treg in tumor tissue of Foxp3$^{YFP\text{-}Cre}$ and CD28 ΔTreg mice at day 17 or 18 after tumor implantation. Data are representative of seven (Foxp3$^{YFP\text{-}Cre}$) and five (CD28 ΔTreg) mice. (**C**) Accumulation of CD28-deficient YFP$^+$ Treg in tumor tissue is more strongly impaired in competitive (CD28 ΔTreg^{het} hosts, $n = 6$) than in noncompetitive settings (CD28 ΔTreg hosts, $n = 5$). CD28-deficient YFP$^+$ Treg were compared with YFP$^+$ Treg in Foxp3$^{YFP\text{-}Cre/wt}$ and Foxp3$^{YFP\text{-}Cre}$ hosts, respectively. Bars show means. The p value was calculated by Mann–Whitney U test. (**D**) Growth of MC38 tumors in CD28 ΔTreg ($n = 4$) mice or Foxp3$^{YFP\text{-}Cre}$ control mice ($n = 6$). Mean ± SEM for are shown. (**E**) Growth of MC38 tumors in mice with inducible Treg-specific deletion of CnB or CD28. Tumor cells were implanted in Foxp3^{CreERT2}, CnB ΔTreg^{ind}, and CD28 ΔTreg^{ind} mice. Arrow indicates start of tamoxifen administration, resulting in the deletion of CnB or CD28. Mean ± SEM for one experiment of two are shown, $n = 4$ per group. (**F**) Growth of MC38 tumors in mixed chimeras generated in irradiated TCRα$^{-/-}$ hosts with Foxp3^{DTR} and CnB ΔTreg, CD28 ΔTreg, or Foxp3$^{YFP\text{-}Cre}$ bone marrow. Upon administration of diphtheria toxin (arrow), mice are acutely converted into functional CnB ΔTreg or CD28 ΔTreg mice without pre-existing lymphoproliferative disease. Foxp3$^{YFP\text{-}Cre}$ + Foxp3^{DTR}: $n = 5$; CnB ΔTreg + Foxp3^{DTR}: $n = 4$; CD28 ΔTreg + Foxp3^{DTR}: $n = 7$. Mean ± SEM are shown. In (A), (D), (E), and (F), $^*p < 0.05$ against control mice, $^{\#}p < 0.05$ against CD28 ΔTreg mice. The p values were calculated using multiple comparison Student t test with Sidak post hoc test.

effectively ablated through diphtheria toxin treatment, acutely creating functional CnB ΔTreg and CD28 ΔTreg mice. When we implanted MC38 colon carcinomas in these animals and initiated diphtheria toxin treatment 4 d later, Foxp3^{DTR} Treg were efficiently deleted (data not shown). As a result, both strains exerted partial control over tumor growth, but control was again more pronounced in mice in which Treg lacked CnB (Fig. 7F). Thus, in two different experimental settings, tumor tolerance was strongly impaired when Treg lacked expression of CnB or CD28. This effect was more pronounced upon deletion of CnB in Treg, correlating with their complete block in eTreg differentiation, whereas loss of CD28 still permits a reduced number of eTreg to enter and function in tumor tissue, explaining the more partial loss of tumor tolerance.

Discussion

In this study, we have defined the respective roles of calcineurin-dependent NFAT activation and CD28 costimulation in the formation and maintenance of effector Treg endowed with the ability to migrate to and accumulate in nonlymphoid tissues, as well as in malignant tumors. We show that cognate Ag encounters in tdLNs activate resting cTreg and enable their clonal expansion and differentiation into eTreg that upregulate markers of elevated suppressive function and chemokine receptors enabling their migration to tumor tissue. In the absence of calcineurin activity, this differentiation process does not occur, and Treg fail to populate tumor and nonlymphoid tissues. Despite residual suppressive activity of CnB-deficient cTreg in vitro, this defect is associated on the one hand with superior immune control of aggressive tumors, but on the other hand with failed immune homeostasis, reflected by an early-onset, rampant lymphoproliferative inflammatory disease replicating the scurfy phenotype. In contrast, eTreg formation still occurs in absence of CD28, but at a diminished rate. Accordingly, a milder form of inflammatory disease occurs only later in life, as previously reported (14–16), accompanied by more variably reduced eTreg accumulation in nonlymphoid tissues. Nevertheless, immune control of aggressive tumors is strongly enhanced.

Our observations consolidate and extend a model in which, under homeostatic conditions, a fraction of Treg in SLOs is continuously exposed to self-antigen–derived TCR ligands, some of which are likely tissue-specific and trigger cTreg differentiation into eTreg capable of entering and persisting in nonlymphoid tissues (3–5, 13, 31, 32). In addition, some nonlymphoid tissues are seeded with

specialized Treg populations soon after birth (56). Based on the complete absence of CnB-deficient Treg in all tested nonlymphoid tissues including the colonic lamina propria, which normally harbors thymically as well as peripherally induced Treg (57), we can conclude that both initial neonatal seeding as well as continued seeding during adult life depend on calcineurin activity subsequent to induction of Foxp3 expression. The requirement for CD28, on the other hand, is much more variable, and very pronounced for instance in skin, but less stringent in lung or colon.

In contrast to normal tissues, tumors rapidly develop de novo in the adult animal. The absence of CnB-deficient Treg at these sites and failed tumor tolerance demonstrate that calcineurin is a key effector of TCR signals that license Treg to populate immune effector sites and regulate ongoing immune responses.

Dendritic cells are known to regulate Treg numbers in an MHC II–dependent manner (58), suggesting a role for direct self-antigen–dependent interactions. However, we found that cTreg numbers in blood and lymphoid tissues and their in vitro–suppressive function are largely preserved in the absence of calcineurin, suggesting that either TCR signals or specifically NFAT activation are not important for maintenance of this subset. This agrees with findings that dendritic cells regulate Treg in SLOs indirectly by activating effector T cells that in turn provide IL-2 to sustain cTreg in a TCR-independent manner (10, 33, 59).

However, cTreg activity does not seem to suffice to maintain systemic immune homeostasis, and the severe inflammatory disease in mice lacking CnB in Treg further underscores the importance of the formation of eTreg with the capacity to traffic to nonlymphoid tissues. Prior studies have shown that deletion of the TCR in mature Treg leads to decreased expression of Foxp3 and of genes important for the suppressive function of eTreg (8). Our observations indicate that calcineurin, and by extension, NFAT proteins, are key drivers of CTLA-4 and ICOS expression. Although induction of Foxp3 expression during Treg development and its maintenance in mature Treg primarily depends on NF-κB proteins, especially c-Rel (60–62), NFAT binding to the CNS2 enhancer element of Foxp3 is important to sustain optimal Foxp3 expression in eTreg (45). NFAT proteins may therefore increase the expression of genes important for Treg-suppressive activity directly through binding on their promoters or regulatory elements, as shown for CTLA-4 and ICOS (44, 63), but also indirectly by optimizing expression of Foxp3. Both of these mechanisms, along with the reported cooperation of NFAT proteins with Foxp3 (64, 65) may thus contribute to the calcineurin-dependent, elevated suppressive function of eTreg triggered by TCR signaling.

In addition to genes closely associated with Treg function, calcineurin-driven NFAT activity also supports Treg proliferation and is essential for the expression of all receptors for nonlymphoid chemokines we have examined. Restricting calcineurin function will therefore not only prevent expansion and optimal suppressive function, but also trafficking of Treg to tumors and to nonlymphoid tissues.

Little is known about the role of TCR-dependent signaling pathways, and in particular of calcineurin or NFAT activity, in the direct regulation of chemokine receptor expression. Prior reports have implicated NFAT proteins in the regulation of CX3CR1 in human PBMCs (66), CCR2 in neurons (67), but also of CXCR5 in follicular Treg, a subset of eTreg (68). Our survey of published chromatin immunoprecipitation sequencing data on NFAT1 binding sites in CD8 T cells (44) revealed that these are frequently located in close proximity to the TSSs of chemokine receptors, especially of the Treg activation–dependent receptors CXCR3, CCR4, and CCR5 studied here. This suggests that in addition to other factors such as T-bet, which has been shown to induce CXCR3 expression in Treg (69), TCR- and calcineurin-dependent NFAT activity is not only critical for expression of these receptors, but also directly drives their expression.

T cells express three NFAT proteins, NFAT1, 2, and 4 (NFATc2, c1, and c3). Compound deletion of either NFAT1 and 2 or 1 and 4 does not abrogate the suppressive function of thymically derived Treg, indicating that expression of either NFAT 2 or 4 by itself suffices to sustain Treg activity. This has led to the conclusion that Treg are less dependent on NFAT than conventional T cells (22, 23), but the absolute requirement for NFAT expression has not been tested. In fact, deletion of all three T cell expression NFAT proteins was necessary to disable NFAT activity in CD8 T cells (44), and it is likely that the same is required to disable NFAT activity in Treg. Our findings demonstrate residual cTreg function, but a complete block in eTreg differentiation in absence of any calcineurin-dependent NFAT activity. Interestingly, Treg that lack CnB can still upregulate CD44 and at least partially downregulate CD62L expression, commonly used markers of eTreg differentiation (3). This shows that some features of T cell activation are preserved in the absence of CnB, whereas other critical aspects of eTreg function are disrupted.

Although calcineurin and NFAT activation were essential for eTreg formation, CD28 appeared to play only an optimizing role. CD28 is essential in Treg development (70), and only conditional deletion in mature Foxp3$^+$ Treg has recently started to reveal the distinct role of CD28 costimulation in their survival and proliferation (14, 71). Extending these prior studies we found that eTreg lacking CD28 were less numerous in tumor-draining LNs and tumor tissue and less numerous or absent in nonlymphoid tissues. This could reflect reduced induction of eTreg differentiation in absence of CD28-mediated amplification of TCR-driven signaling pathways. Because Treg express TCRs with a range of peptide–MHC affinities, only those Treg with the highest TCR affinity may be activated in the absence of costimulation. This in turn would lead to a narrowing of the eTreg repertoire, which has been shown to increase the propensity for autoimmune disease (72). Alternatively, Treg may be activated at normal efficiency, but their proliferation or the survival of proliferating cells is reduced as a result of impaired induction of CD28-dependent survival factors (73) or metabolic adaptation (74). Impaired survival may be compounded by reduced expression of ICOS, which promotes eTreg survival in IL-2–poor environments, such as in tumor tissue (3). The fact that the frequency of CD28-deficient Treg was more severely decreased in tumors and in nonlymphoid tissues than in SLOs, and that CD28-deficient Treg were more compromised in tumors when they were in competition with CD28-sufficient Treg, argues for a reduction in fitness.

One of the central functions of CD28 costimulation in synergy with TCR signals is to facilitate robust NF-κB activation via the PDK1/PKCθ/CARMA1 pathway (55). Interestingly, the phenotype of mild lymphoproliferative disease and impaired tumor tolerance in CD28 ΔTreg mice resembles that in mice with Treg-specific conditional deletion of the NF-κB protein c-Rel (62), suggesting that impaired c-Rel activation may account in large part for the defects in CD28-deficient Treg. c-Rel is partially redundant with the NF-κB protein p65/RelA, and deletion of both proteins in Treg is required to produce the scurfy phenotype (62). RelA appears to be more effectively activated in Treg by members of the TNF receptor superfamily, such as GITR, than by the TCR (75), probably explaining why CD28-deficient Treg do not exhibit more severe defects, despite the virtually complete block in NF-κB activation we observed upon TCR activation in vitro.

Do CD28 and calcineurin signals synergize or promote eTreg function independently? PKCθ and Akt, which are both regulated by CD28 signaling, can prolong NFAT activation through inhibition of GSK3β, which phosphorylates NFAT and thereby accelerates its inactivation (76). However, we did not observe any defect in NFAT nuclear translocation in CD28-deficient Treg, suggesting that at least in Treg, CD28 was instead most important for the activity of calcineurin-independent signaling pathways, such as NF-κB activation via PKCθ. Conversely, lack of calcineurin did not attenuate CD28-regulated activities, such as ERK, mTORC1, and NF-κB signaling. In this regard one should also note that, although individual deletion of the NF-κB proteins c-Rel and RelA in Treg produced less severe disease, their compound deletion produced a scurfy phenotype similar to the one we observe in CnB ΔTreg mice. However, the entire Treg compartment appears to be destabilized in the animals, resulting in expression of effector T cell genes (62), in contrast to the selective block in cTreg to eTreg differentiation and the failure to accumulate in nonlymphoid tissues in the absence of CnB. Thus, calcineurin on the one hand and CD28 and NF-κB proteins on the other hand likely support eTreg formation and function through different mechanisms in Treg.

Understanding the roles of various TCR- and costimulation-dependent signaling pathways in regulating the formation and function of eTreg has the potential to inform strategies for their therapeutic manipulation to antagonize their tumor tolerance–supporting function without systemic disruption of immunological self-tolerance in cancer patients. Our findings demonstrate that an absolute block in eTreg formation in the absence of CnB results in immune control of highly aggressive tumors. This is reminiscent of the long-standing observation that calcineurin inhibitors prevent the formation of long-term immune tolerance to transplanted allogeneic solid organs (77). Although prior efforts to therapeutically target a toxin to Treg via CD25 have not been successful in cancer patients (78), likely at least in part because of insufficient selectivity of CD25 expression on Treg, other cell surface proteins, such as the chemokine receptors CCR4 and CCR8, have recently been described to be more selectively expressed on tumor-reactive eTreg (42, 43, 79). It may be possible to use these receptors for Treg-specific delivery of calcineurin inhibitors to Treg to curb tumor growth.

In contrast to calcineurin, CD28 costimulation seems to continually optimize the fitness of eTreg in nonlymphoid tissue, given their more dramatic decline at these sites compared with SLOs, and selectively antagonizing CD28 in Treg will likely directly affect already formed eTreg, including those in tumor tissue. Several studies have already shown how disruption in Treg of individual CD28-driven pathways, such as PI3K signaling (80), Akt-dependent Foxo1 inactivation (6), and, more recently, c-Rel (81), can promote tumor control. The capability to antagonize these pathways or CD28 itself selectively in Treg may dictate in part which target will have the greatest utility in cancer immunotherapy in the future.

Acknowledgments

We thank Jason McCarthy, Esteban Carrizosa, Mauro Di Pilato, Jasper Pruessmann, and Shariq Usmani and the Massachusetts General Hospital Department of Pathology Flow and Image Cytometry Research Core for helpful discussions and technical support.

Disclosures

The authors have no financial conflicts of interest.

References

1. Gajewski, T. F., Y. Meng, C. Blank, I. Brown, A. Kacha, J. Kline, and H. Harlin. 2006. Immune resistance orchestrated by the tumor microenvironment. *Immunol. Rev.* 213: 131–145.
2. Huehn, J., K. Siegmund, J. C. U. Lehmann, C. Siewert, U. Haubold, M. Feuerer, G. F. Debes, J. Lauber, O. Frey, G. K. Przybylski, et al. 2004. Developmental stage, phenotype, and migration distinguish naive- and effector/memory-like CD4+ regulatory T cells. *J. Exp. Med.* 199: 303–313.
3. Smigiel, K. S., E. Richards, S. Srivastava, K. R. Thomas, J. C. Dudda, K. D. Klonowski, and D. J. Campbell. 2014. CCR7 provides localized access to IL-2 and defines homeostatically distinct regulatory T cell subsets. *J. Exp. Med.* 211: 121–136.
4. Fisson, S., G. Darrasse-Jèze, E. Litvinova, F. Septier, D. Klatzmann, R. Liblau, and B. L. Salomon. 2003. Continuous activation of autoreactive CD4+ CD25+ regulatory T cells in the steady state. *J. Exp. Med.* 198: 737–746.
5. Darrasse-Jèze, G., A.-S. Bergot, A. Durgeau, F. Billiard, B. L. Salomon, J. L. Cohen, B. Bellier, K. Podsypanina, and D. Klatzmann. 2009. Tumor emergence is sensed by self-specific CD44hi memory Tregs that create a dominant tolerogenic environment for tumors in mice. *J. Clin. Invest.* 119: 2648–2662.
6. Luo, C. T., W. Liao, S. Dadi, A. Toure, and M. O. Li. 2016. Graded Foxo1 activity in Treg cells differentiates tumour immunity from spontaneous autoimmunity. *Nature* 529: 532–536.
7. Bauer, C. A., E. Y. Kim, F. Marangoni, E. Carrizosa, N. M. Claudio, and T. R. Mempel. 2014. Dynamic Treg interactions with intratumoral APCs promote local CTL dysfunction. *J. Clin. Invest.* 124: 2425–2440.
8. Levine, A. G., A. Arvey, W. Jin, and A. Y. Rudensky. 2014. Continuous requirement for the TCR in regulatory T cell function. *Nat. Immunol.* 15: 1070–1078.
9. Vahl, J. C., C. Drees, K. Heger, S. Heink, J. C. Fischer, J. Nedjic, N. Ohkura, H. Morikawa, H. Poeck, S. Schallenberg, et al. 2014. Continuous T cell receptor signals maintain a functional regulatory T cell pool. *Immunity* 41: 722–736.
10. Barron, L., H. Dooms, K. K. Hoyer, W. Kuswanto, J. Hofmann, W. E. O'Gorman, and A. K. Abbas. 2010. Cutting edge: mechanisms of IL-2-dependent maintenance of functional regulatory T cells. *J. Immunol.* 185: 6426–6430.
11. Lee, J. H., S. G. Kang, and C. H. Kim. 2007. FoxP3+ T cells undergo conventional first switch to lymphoid tissue homing receptors in thymus but accelerated second switch to nonlymphoid tissue homing receptors in secondary lymphoid tissues. *J. Immunol.* 178: 301–311.
12. O'Gorman, W. E., H. Dooms, S. H. Thorne, W. F. Kuswanto, E. F. Simonds, P. O. Krutzik, G. P. Nolan, and A. K. Abbas. 2009. The initial phase of an immune response functions to activate regulatory T cells. *J. Immunol.* 183: 332–339.
13. Sather, B. D., P. Treuting, N. Perdue, M. Miazgowicz, J. D. Fontenot, A. Y. Rudensky, and D. J. Campbell. 2007. Altering the distribution of Foxp3(+) regulatory T cells results in tissue-specific inflammatory disease. *J. Exp. Med.* 204: 1335–1347.
14. Zhang, R., A. Huynh, G. Whitcher, J. Chang, J. S. Maltzman, and L. A. Turka. 2013. An obligate cell-intrinsic function for CD28 in Tregs. *J. Clin. Invest.* 123: 580–593.
15. Zhang, R., C. M. Borges, M. Y. Fan, J. E. Harris, and L. A. Turka. 2015. Requirement for CD28 in effector regulatory T cell differentiation, CCR6 induction, and skin homing. *J. Immunol.* 195: 4154–4161.
16. Zhang, R., P. T. Sage, K. Finn, A. Huynh, B. R. Blazar, F. Marangoni, T. R. Mempel, A. H. Sharpe, and L. A. Turka. 2017. B cells drive autoimmunity in mice with CD28-deficient regulatory T cells. *J. Immunol.* 199: 3972–3980.
17. Gavin, M. A., S. R. Clarke, E. Negrou, A. Gallegos, and A. Rudensky. 2002. Homeostasis and anergy of CD4(+)CD25(+) suppressor T cells in vivo. *Nat. Immunol.* 3: 33–41.
18. Hickman, S. P., J. Yang, R. M. Thomas, A. D. Wells, and L. A. Turka. 2006. Defective activation of protein kinase C and Ras-ERK pathways limits IL-2 production and proliferation by CD4+CD25+ regulatory T cells. *J. Immunol.* 177: 2186–2194.
19. Yan, D., J. Farache, M. Mingueneau, D. Mathis, and C. Benoist. 2015. Imbalanced signal transduction in regulatory T cells expressing the transcription factor FoxP3. [Published erratum appears in 2016 *Proc. Natl. Acad. Sci. USA* 113: E256.] *Proc. Natl. Acad. Sci. USA* 112: 14942–14947.
20. Zeiser, R., V. H. Nguyen, A. Beilhack, M. Buess, S. Schulz, J. Baker, C. H. Contag, and R. S. Negrin. 2006. Inhibition of CD4+CD25+ regulatory T-cell function by calcineurin-dependent interleukin-2 production. *Blood* 108: 390–399.
21. Bopp, T., A. Palmetshofer, E. Serfling, V. Heib, S. Schmitt, C. Richter, M. Klein, H. Schild, E. Schmitt, and M. Stassen. 2005. NFATc2 and NFATc3 transcription factors play a crucial role in suppression of CD4+ T lymphocytes by CD4+ CD25+ regulatory T cells. *J. Exp. Med.* 201: 181–187.
22. Vaeth, M., U. Schliesser, G. Müller, S. Reissig, K. Satoh, A. Tuettenberg, H. Jonuleit, A. Waisman, M. R. Müller, E. Serfling, et al. 2012. Dependence on nuclear factor of activated T-cells (NFAT) levels discriminates conventional T cells from Foxp3+ regulatory T cells. *Proc. Natl. Acad. Sci. USA* 109: 16258–16263.
23. Vaeth, M., C. A. Bäuerlein, T. Pusch, J. Findeis, M. Chopra, A. Mottok, A. Rosenwald, A. Beilhack, and F. Berberich-Siebelt. 2015. Selective NFAT targeting in T cells ameliorates GvHD while maintaining antitumor activity. *Proc. Natl. Acad. Sci. USA* 112: 1125–1130.

24. Li, Q., A. Shakya, X. Guo, H. Zhang, D. Tantin, P. E. Jensen, and X. Chen. 2012. Constitutive nuclear localization of NFAT in Foxp3+ regulatory T cells independent of calcineurin activity. *J. Immunol.* 188: 4268–4277.
25. Sumpter, T. L., K. K. Payne, and D. S. Wilkes. 2008. Regulation of the NFAT pathway discriminates CD4+CD25+ regulatory T cells from CD4+CD25- helper T cells. *J. Leukoc. Biol.* 83: 708–717.
26. Neilson, J. R., M. M. Winslow, E. M. Hur, and G. R. Crabtree. 2004. Calcineurin B1 is essential for positive but not negative selection during thymocyte development. *Immunity* 20: 255–266.
27. Rubtsov, Y. P., J. P. Rasmussen, E. Y. Chi, J. Fontenot, L. Castelli, X. Ye, P. Treuting, L. Siewe, A. Roers, W. R. Henderson, Jr., et al. 2008. Regulatory T cell-derived interleukin-10 limits inflammation at environmental interfaces. *Immunity* 28: 546–558.
28. Rubtsov, Y. P., R. E. Niec, S. Josefowicz, L. Li, J. Darce, D. Mathis, C. Benoist, and A. Y. Rudensky. 2010. Stability of the regulatory T cell lineage in vivo. *Science* 329: 1667–1671.
29. Kim, J. M., J. P. Rasmussen, and A. Y. Rudensky. 2007. Regulatory T cells prevent catastrophic autoimmunity throughout the lifespan of mice. *Nat. Immunol.* 8: 191–197.
30. Marangoni, F., T. T. Murooka, T. Manzo, E. Y. Kim, E. Carrizosa, N. M. Elpek, and T. R. Mempel. 2013. The transcription factor NFAT exhibits signal memory during serial T cell interactions with antigen-presenting cells. *Immunity* 38: 237–249.
31. Samy, E. T., L. A. Parker, C. P. Sharp, and K. S. K. Tung. 2005. Continuous control of autoimmune disease by antigen-dependent polyclonal CD4+CD25+ regulatory T cells in the regional lymph node. [Published erratum appears in 2005 *J. Exp. Med.* 202: 1153.] *J. Exp. Med.* 202: 771–781.
32. Setiady, Y. Y., K. Ohno, E. T. Samy, H. Bagavant, H. Qiao, C. Sharp, J. X. She, and K. S. K. Tung. 2006. Physiologic self antigens rapidly capacitate autoimmune disease-specific polyclonal CD4+ CD25+ regulatory T cells. *Blood* 107: 1056–1062.
33. Liu, Z., M. Y. Gerner, N. Van Panhuys, A. G. Levine, A. Y. Rudensky, and R. N. Germain. 2015. Immune homeostasis enforced by co-localized effector and regulatory T cells. *Nature* 528: 225–230.
34. Carrizosa, E., and T. R. Mempel. 2015. Immunology: in the right place at the right time. *Nature* 528: 205–206.
35. Lio, C.-W. J., and C.-S. Hsieh. 2008. A two-step process for thymic regulatory T cell development. *Immunity* 28: 100–111.
36. Godfrey, V. L., J. E. Wilkinson, E. M. Rinchik, and L. B. Russell. 1991. Fatal lymphoreticular disease in the *scurfy* (sf) mouse requires T cells that mature in a sf thymic environment: potential model for thymic education. *Proc. Natl. Acad. Sci. USA* 88: 5528–5532.
37. Fontenot, J. D., M. A. Gavin, and A. Y. Rudensky. 2003. Foxp3 programs the development and function of CD4+CD25+ regulatory T cells. *Nat. Immunol.* 4: 330–336.
38. Weninger, W., M. A. Crowley, N. Manjunath, and U. H. von Andrian. 2001. Migratory properties of naive, effector, and memory CD8(+) T cells. *J. Exp. Med.* 194: 953–966.
39. Semprini, S., T. J. Troup, N. Kotelevtseva, K. King, J. R. E. Davis, L. J. Mullins, K. E. Chapman, D. R. Dunbar, and J. J. Mullins. 2007. Cryptic loxP sites in mammalian genomes: genome-wide distribution and relevance for the efficiency of BAC/PAC recombineering techniques. *Nucleic Acids Res.* 35: 1402–1410.
40. Delgoffe, G. M., S.-R. Woo, M. E. Turnis, D. M. Gravano, C. Guy, A. E. Overacre, M. L. Bettini, P. Vogel, D. Finkelstein, J. Bonnevier, et al. 2013. Stability and function of regulatory T cells is maintained by a neuropilin-1-semaphorin-4a axis. *Nature* 501: 252–256.
41. Liu, Y., L. Wang, J. Predina, R. Han, U. H. Beier, L.-C. S. Wang, V. Kapoor, T. R. Bhatti, T. Akimova, S. Singhal, et al. 2013. Inhibition of p300 impairs Foxp3$^+$ T regulatory cell function and promotes antitumor immunity. *Nat. Med.* 19: 1173–1177.
42. De Simone, M., A. Arrigoni, G. Rossetti, P. Gruarin, V. Ranzani, C. Politano, R. J. P. Bonnal, E. Provasi, M. L. Sarnicola, I. Panzeri, et al. 2016. Transcriptional landscape of human tissue lymphocytes unveils uniqueness of tumor-infiltrating T regulatory cells. *Immunity* 45: 1135–1147.
43. Plitas, G., C. Konopacki, K. Wu, P. D. Bos, M. Morrow, E. V. Putintseva, D. M. Chudakov, and A. Y. Rudensky. 2016. Regulatory T cells exhibit distinct features in human breast cancer. *Immunity* 45: 1122–1134.
44. Martinez, G. J., R. M. Pereira, T. Äijö, E. Y. Kim, F. Marangoni, M. E. Pipkin, S. Togher, V. Heissmeyer, Y. C. Zhang, S. Crotty, et al. 2015. The transcription factor NFAT promotes exhaustion of activated CD8$^+$ T cells. *Immunity* 42: 265–278.
45. Li, X., Y. Liang, M. LeBlanc, C. Benner, and Y. Zheng. 2014. Function of a Foxp3 cis-element in protecting regulatory T cell identity. *Cell* 158: 734–748.
46. Redjimi, N., C. Raffin, I. Raimbaud, P. Pignon, J. Matsuzaki, K. Odunsi, D. Valmori, and M. Ayyoub. 2012. CXCR3+ T regulatory cells selectively accumulate in human ovarian carcinomas to limit type I immunity. *Cancer Res.* 72: 4351–4360.
47. Tan, M. C. B., P. S. Goedegebuure, B. A. Belt, B. Flaherty, N. Sankpal, W. E. Gillanders, T. J. Eberlein, C.-S. Hsieh, and D. C. Linehan. 2009. Disruption of CCR5-dependent homing of regulatory T cells inhibits tumor growth in a murine model of pancreatic cancer. *J. Immunol.* 182: 1746–1755.
48. Curiel, T. J., G. Coukos, L. Zou, X. Alvarez, P. Cheng, P. Mottram, M. Evdemon-Hogan, J. R. Conejo-Garcia, L. Zhang, M. Burow, et al. 2004. Specific recruitment of regulatory T cells in ovarian carcinoma fosters immune privilege and predicts reduced survival. *Nat. Med.* 10: 942–949.
49. Wing, K., Y. Onishi, P. Prieto-Martin, T. Yamaguchi, M. Miyara, Z. Fehervari, T. Nomura, and S. Sakaguchi. 2008. CTLA-4 control over Foxp3+ regulatory T cell function. *Science* 322: 271–275.
50. Patra, A. K., A. Avots, R. P. Zahedi, T. Schüler, A. Sickmann, U. Bommhardt, and E. Serfling. 2013. An alternative NFAT-activation pathway mediated by IL-7 is critical for early thymocyte development. *Nat. Immunol.* 14: 127–135.
51. Palkowitsch, L., U. Marienfeld, C. Brunner, A. Eitelhuber, D. Krappmann, and R. B. Marienfeld. 2011. The Ca2+-dependent phosphatase calcineurin controls the formation of the Carma1-Bcl10-Malt1 complex during T cell receptor-induced NF-kappaB activation. *J. Biol. Chem.* 286: 7522–7534.
52. Diehn, M., A. A. Alizadeh, O. J. Rando, C. L. Liu, K. Stankunas, D. Botstein, G. R. Crabtree, and P. O. Brown. 2002. Genomic expression programs and the integration of the CD28 costimulatory signal in T cell activation. [Published erratum appears in 2002 *Proc. Natl. Acad. Sci. USA* 99: 15245.] *Proc. Natl. Acad. Sci. USA* 99: 11796–11801.
53. Michel, F., G. Attal-Bonnefoy, G. Mangino, S. Mise-Omata, and O. Acuto. 2001. CD28 as a molecular amplifier extending TCR ligation and signaling capabilities. *Immunity* 15: 935–945.
54. Narayan, P., B. Holt, R. Tosti, and L. P. Kane. 2006. CARMA1 is required for Akt-mediated NF-kappaB activation in T cells. *Mol. Cell. Biol.* 26: 2327–2336.
55. Park, S.-G., J. Schulze-Luehrman, M. S. Hayden, N. Hashimoto, W. Ogawa, M. Kasuga, and S. Ghosh. 2009. The kinase PDK1 integrates T cell antigen receptor and CD28 coreceptor signaling to induce NF-kappaB and activate T cells. *Nat. Immunol.* 10: 158–166.
56. Scharschmidt, T. C., K. S. Vasquez, H.-A. Truong, S. V. Gearty, M. L. Pauli, A. Nosbaum, I. K. Gratz, M. Otto, J. J. Moon, J. Liese, et al. 2015. A wave of regulatory T cells into neonatal skin mediates tolerance to commensal microbes. *Immunity* 43: 1011–1021.
57. Cebula, A., M. Seweryn, G. A. Rempala, S. S. Pabla, R. A. McIndoe, T. L. Denning, L. Bry, P. Kraj, P. Kisielow, and L. Ignatowicz. 2013. Thymus-derived regulatory T cells contribute to tolerance to commensal microbiota. *Nature* 497: 258–262.
58. Darrasse-Jèze, G., S. Deroubaix, H. Mouquet, G. D. Victora, T. Eisenreich, K.-H. Yao ,R. F. Masilamani, M. L. Dustin, A. Rudensky, K. Liu, and M. C. Nussenzweig. 2009. Feedback control of regulatory T cell homeostasis by dendritic cells in vivo. *J. Exp. Med.* 206: 1853–1862.
59. Stolley, J. M., and D. J. Campbell. 2016. A 33D1+ dendritic cell/autoreactive CD4+ T cell circuit maintains IL-2-dependent regulatory T cells in the spleen. *J. Immunol.* 197: 2635–2645.
60. Long, M., S.-G. Park, I. Strickland, M. S. Hayden, and S. Ghosh. 2009. Nuclear factor-kappaB modulates regulatory T cell development by directly regulating expression of Foxp3 transcription factor. *Immunity* 31: 921–931.
61. Ruan, Q., V. Kameswaran, Y. Tone, L. Li, H.-C. Liou, M. I. Greene, M. Tone, and Y. H. Chen. 2009. Development of Foxp3(+) regulatory t cells is driven by the c-Rel enhanceosome. *Immunity* 31: 932–940.
62. Oh, H., Y. Grinberg-Bleyer, W. Liao, D. Maloney, P. Wang, Z. Wu, J. Wang, D. M. Bhatt, N. Heise, R. M. Schmid, et al. 2017. An NF-κB transcription-factor-dependent lineage-specific transcriptional program promotes regulatory T cell identity and function. *Immunity* 47: 450–465.e5.
63. Martinez, G. J., J. K. Hu, R. M. Pereira, J. S. Crampton, S. Togher, N. Bild, S. Crotty, and A. Rao. 2016. Cutting edge: NFAT transcription factors promote the generation of follicular helper T cells in response to acute viral infection. *J. Immunol.* 196: 2015–2019.
64. Samstein, R. M., A. Arvey, S. Z. Josefowicz, X. Peng, A. Reynolds, R. Sandstrom, S. Neph, P. Sabo, J. M. Kim, W. Liao, et al. 2012. Foxp3 exploits a pre-existent enhancer landscape for regulatory T cell lineage specification. *Cell* 151: 153–166.
65. Wu, Y., M. Borde, V. Heissmeyer, M. Feuerer, A. D. Lapan, J. C. Stroud, D. L. Bates, L. Guo, A. Han, S. F. Ziegler, et al. 2006. FOXP3 controls regulatory T cell function through cooperation with NFAT. *Cell* 126: 375–387.
66. Barlic, J., D. H. McDermott, M. N. Merrell, J. Gonzales, L. E. Via, and P. M. Murphy. 2004. Interleukin (IL)-15 and IL-2 reciprocally regulate expression of the chemokine receptor CX3CR1 through selective NFAT1- and NFAT2-dependent mechanisms. *J. Biol. Chem.* 279: 48520–48534.
67. Jung, H., and R. J. Miller. 2008. Activation of the nuclear factor of activated T-cells (NFAT) mediates upregulation of CCR2 chemokine receptors in dorsal root ganglion (DRG) neurons: a possible mechanism for activity-dependent transcription in DRG neurons in association with neuropathic pain. *Mol. Cell. Neurosci.* 37: 170–177.
68. Vaeth, M., G. Müller, D. Stauss, L. Dietz, S. Klein-Hessling, E. Serfling, M. Lipp, I. Berberich, and F. Berberich-Siebelt. 2014. Follicular regulatory T cells control humoral autoimmunity via NFAT2-regulated CXCR5 expression. *J. Exp. Med.* 211: 545–561.
69. Koch, M. A., G. Tucker-Heard, N. R. Perdue, J. R. Killebrew, K. B. Urdahl, and D. J. Campbell. 2009. The transcription factor T-bet controls regulatory T cell homeostasis and function during type 1 inflammation. *Nat. Immunol.* 10: 595–602.
70. Salomon, B., D. J. Lenschow, L. Rhee, N. Ashourian, B. Singh, A. Sharpe, and J. A. Bluestone. 2000. B7/CD28 costimulation is essential for the homeostasis of the CD4+CD25+ immunoregulatory T cells that control autoimmune diabetes. *Immunity* 12: 431–440.
71. Gogishvili, T., F. Lühder, S. Goebbels, S. Beer-Hammer, K. Pfeffer, and T. Hünig. 2013. Cell-intrinsic and -extrinsic control of Treg-cell homeostasis and function revealed by induced CD28 deletion. *Eur. J. Immunol.* 43: 188–193.

72. Feng, Y., J. van der Veeken, M. Shugay, E. V. Putintseva, H. U. Osmanbeyoglu, S. Dikiy, B. E. Hoyos, B. Moltedo, S. Hemmers, P. Treuting, et al. 2015. A mechanism for expansion of regulatory T-cell repertoire and its role in self-tolerance. *Nature* 528: 132–136.
73. Boise, L. H., A. J. Minn, P. J. Noel, C. H. June, M. A. Accavitti, T. Lindsten, and C. B. Thompson. 1995. CD28 costimulation can promote T cell survival by enhancing the expression of Bcl-XL. *Immunity* 3: 87–98.
74. Frauwirth, K. A., J. L. Riley, M. H. Harris, R. V. Parry, J. C. Rathmell, D. R. Plas, R. L. Elstrom, C. H. June, and C. B. Thompson. 2002. The CD28 signaling pathway regulates glucose metabolism. *Immunity* 16: 769–777.
75. Vasanthakumar, A., Y. Liao, P. Teh, M. F. Pascutti, A. E. Oja, A. L. Garnham, R. Gloury, J. C. Tempany, T. Sidwell, E. Cuadrado, et al. 2017. The TNF receptor superfamily-NF-κB axis is critical to maintain effector regulatory T cells in lymphoid and non-lymphoid tissues. *Cell Reports* 20: 2906–2920.
76. Beals, C. R., C. M. Sheridan, C. W. Turck, P. Gardner, and G. R. Crabtree. 1997. Nuclear export of NF-ATc enhanced by glycogen synthase kinase-3. *Science* 275: 1930–1934.
77. Li, Y., X. C. Li, X. X. Zheng, A. D. Wells, L. A. Turka, and T. B. Strom. 1999. Blocking both signal 1 and signal 2 of T-cell activation prevents apoptosis of alloreactive T cells and induction of peripheral allograft tolerance. *Nat. Med.* 5: 1298–1302.
78. Luke, J. J., Y. Zha, K. Matijevich, and T. F. Gajewski. 2016. Single dose denileukin diftitox does not enhance vaccine-induced T cell responses or effectively deplete Tregs in advanced melanoma: immune monitoring and clinical results of a randomized phase II trial. *J. Immunother. Cancer* 4: 35.
79. Sugiyama, D., H. Nishikawa, Y. Maeda, M. Nishioka, A. Tanemura, I. Katayama, S. Ezoe, Y. Kanakura, E. Sato, Y. Fukumori, et al. 2013. Anti-CCR4 mAb selectively depletes effector-type FoxP3+CD4+ regulatory T cells, evoking antitumor immune responses in humans. *Proc. Natl. Acad. Sci. USA* 110: 17945–17950.
80. Ali, K., D. R. Soond, R. Piñeiro, T. Hagemann, W. Pearce, E. L. Lim, H. Bouabe, C. L. Scudamore, T. Hancox, H. Maecker, et al. 2014. Inactivation of PI(3)K p110δ breaks regulatory T-cell-mediated immune tolerance to cancer. *Nature* 510: 407–411.
81. Grinberg-Bleyer, Y., H. Oh, A. Desrichard, D. M. Bhatt, R. Caron, T. A. Chan, R. M. Schmid, U. Klein, M. S. Hayden, and S. Ghosh. 2017. NF-κB c-Rel is crucial for the regulatory T cell immune checkpoint in cancer. *Cell* 170: 1096–1108.e13.

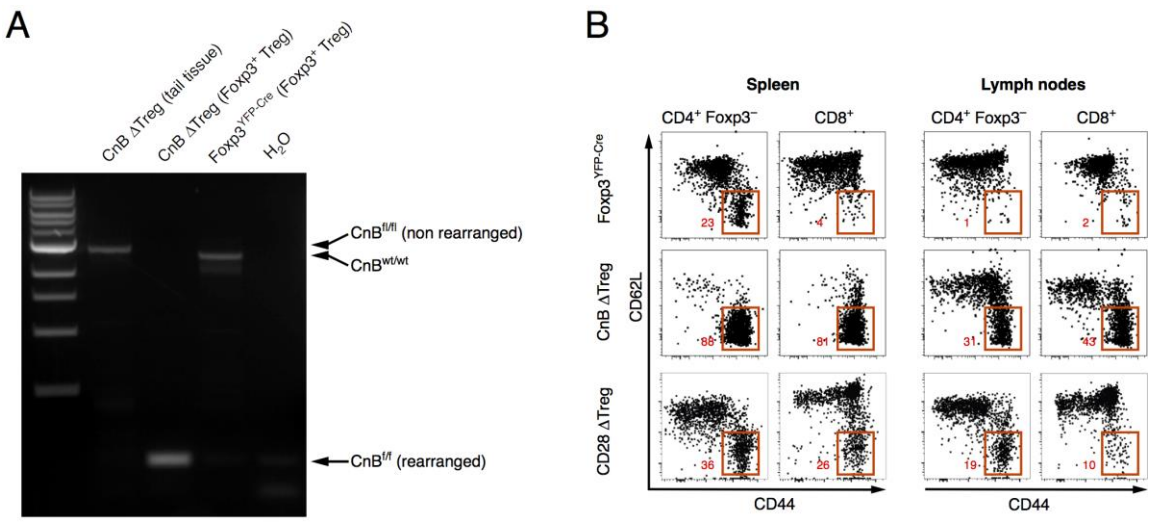

Figure S1: Treg-specific deletion of CnB or CD28 leads to expansion of effector T cells. (A) PCR analysis of the CnB locus in non-lymphoid tissue (tail) and Treg from CnB ΔTreg and Foxp3$^{YFP\text{-}Cre}$ mice. Note the complete deletion of the floxed CnB alleles in Tregs isolated from CnB ΔTreg mice. (B) Expression of CD62L and CD44 on CD4^{+} FoxP3^{-} or CD8^{+} conventional T cells. Note the expansion of T cells with a CD44^{hi} CD62L^{neg} effector/effector memory phenotype.

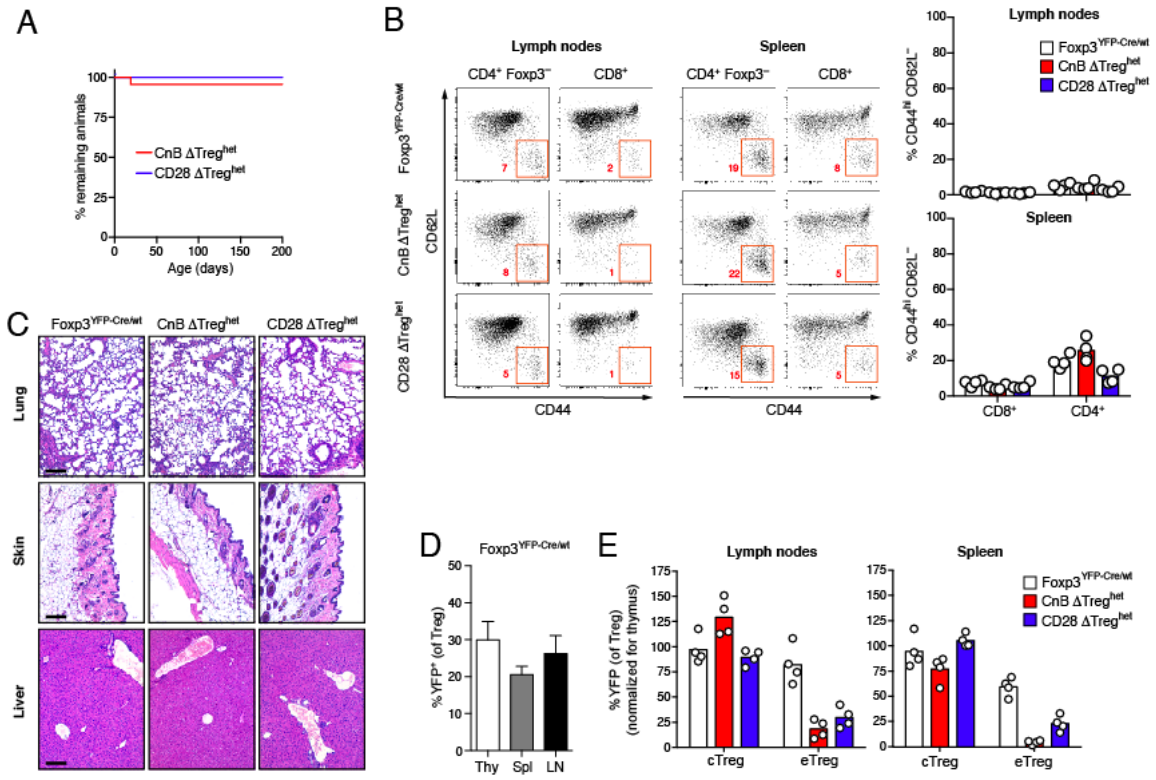

Figure S2: CnB ΔTreg^{het} and CD28 ΔTreg^{het} mice are healthy and show no signs of lymphoproliferative disease. (A) Survival curves of CnB ΔTreg^{het} (n=23) and CD28 ΔTreg^{het} (n=14) mice. (B) CD44 and CD62L expression on CD8^{+} and CD4^{+} conventional T cells in 5 month-old mice. Note the lack of expansion of conventional T cells with the CD44^{hi} CD62L^{-} effector phenotype. (C) H&E-stained sections of lung, skin and liver of the indicated mice. Bars equal 200 μm. (D) Treg expressing the Foxp3$^{YFP-Cre}$ allele are under-represented relative to their YFP-Cre^{neg} counterparts in thymus, LNs and spleen of Foxp3$^{YFP-Cre/wt}$ control mice. Their frequency is significantly lower than 50%, as determined by one-sample t-test ($p<0.05$), in all organs examined. Mean and SD is shown, n=3. (E) The percentage of YFP^{+} cTreg or eTreg in LNs and spleen was normalized to their percentage in the thymus. This revealed a selective disadvantage for cells lacking CnB or CD28 during the differentiation from central to effector Treg, irrespective of anatomical site.

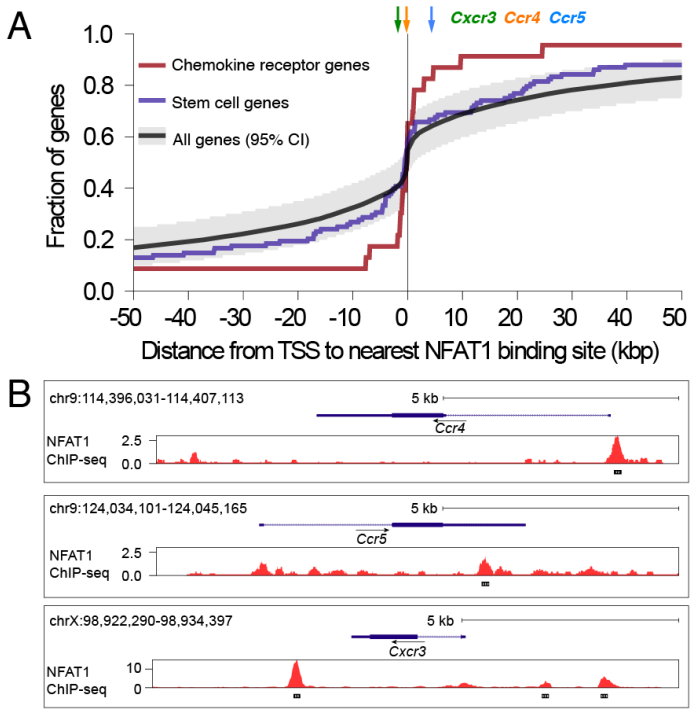

C

Gene	Distance to closest NFAT1 peak (bp)
Cxcr7	-261636
Pitpnm3	-79357
Darc	-40621
Ccbp2	-7664
Xcr1	-7521
Cxcr1	-6895
Cxcr3	-1763
Cxcr6	-1309
Ccr1l1	-1278
Ccr9	-937
Ccr8	-833
Ccr10	-395
Cxcr4	-291
Ccr4	-72
Cxcr5	-68
Cx3cr1	0
Ccr1	0
Ccr7	971
Ccr3	1188
Ccr2	1273
Ccr6	3051
Ccr5	4709
Ccrl2	9742
Cxcr2	24680
Ccrl1	50662

Figure S3: Transcription starts sites of chemokine receptor genes are positioned close to NFAT1-binding sites. (A) A published CHIP-Seq data set of NFAT1 binding sites in mouse $CD8^+$ T cells (Martinez G.J. et al, *Immunity*, 2015) was parsed to determine the cumulative distribution of distances of transcription start sites (TSS) site of chemokine receptor genes, stem cell genes, and all genes analyzed to the nearest NFAT1 binding site. TSS-NFAT1 binding site distances for Ccr4, Ccr5 and Cxcr3 are annotated by arrows. (B) Genome browser views of the Ccr4, Ccr5 and Cxcr3 loci showing the distribution of NFAT1 CHIP-Seq peaks. Blue diagram: gene transcript; thin lines: introns; thick lines: exons; thickest lines: coding regions. Red histogram: CHIP-Seq peak distribution; black underscores: CHIP-Seq peak annotation. (C) List of distances from each chemokine receptor gene TSS to the closest NFAT1 peak.

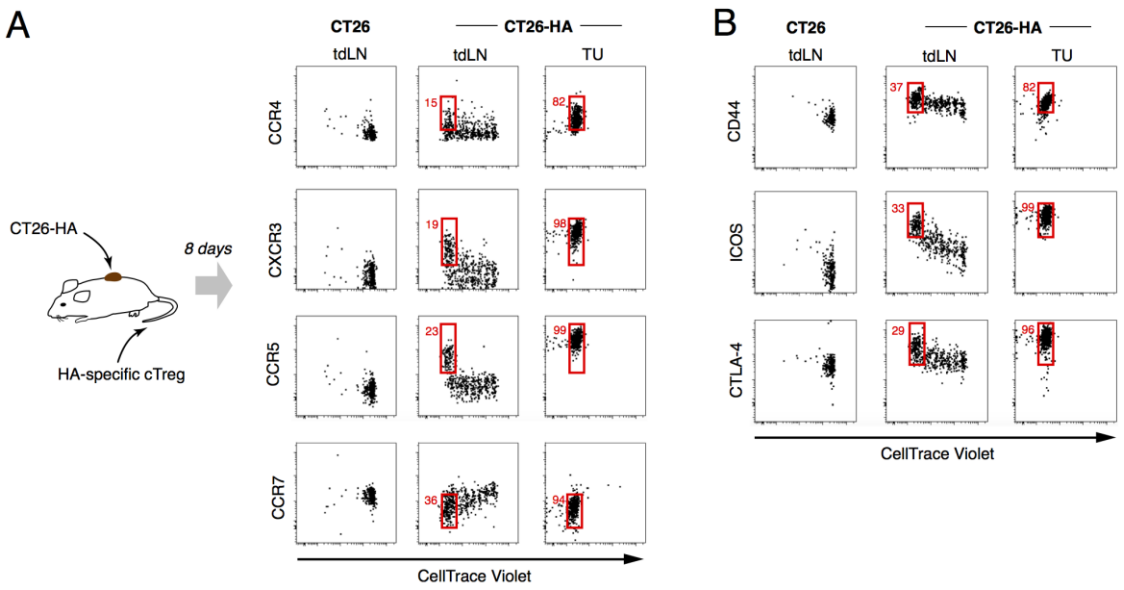

Figure S4: Differentiation of tumor-homing eTreg is antigen dependent.

Hemagglutinin (HA)-specific cTreg were labeled with CellTrace Violet and adoptively transferred into BALB/c mice, which were subsequently injected with CT26 colon carcinoma cells engineered to express HA (CT26-HA), or with CT26 control tumors. Eight days later, cellular proliferation and expression of the chemokine receptors CCR4, CXCR3, CCR5 and CCR7 (A), or CD44, ICOS, and CTLA-4 (B) was measured in tumor-draining LNs and in tumor tissue. HA-specific Treg gradually acquired immunophenotypic characteristics of tumor-homing eTreg in an antigen-dependent way and accumulated in HA-expressing tumors.